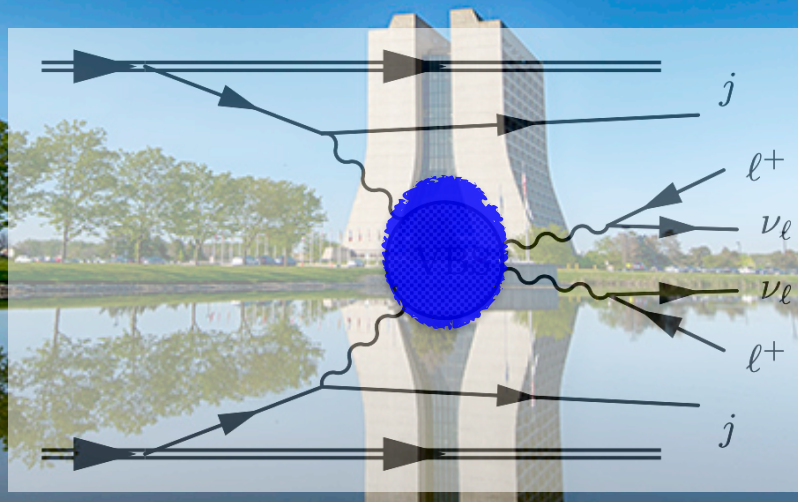


EFT in Multiboson physics at CMS



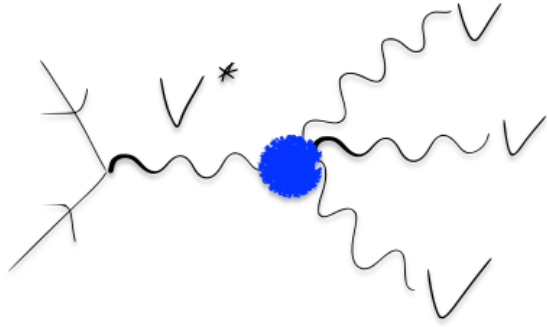
Irene Zoi

CMS EFT workshop at the LPC, September 2023

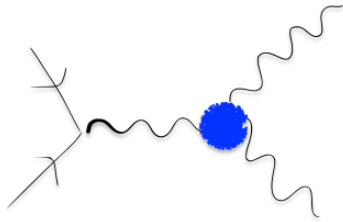


The SM (and beyond?) physics processes

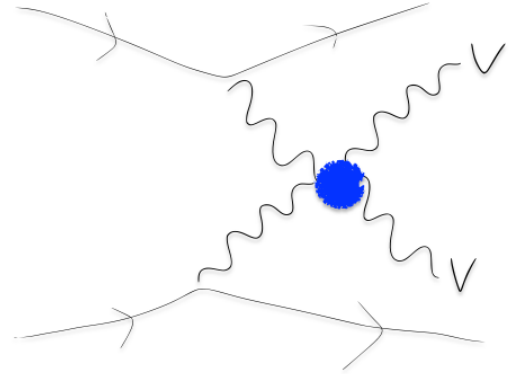
Triboson



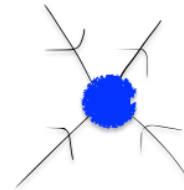
Diboson



Vector Boson Scattering

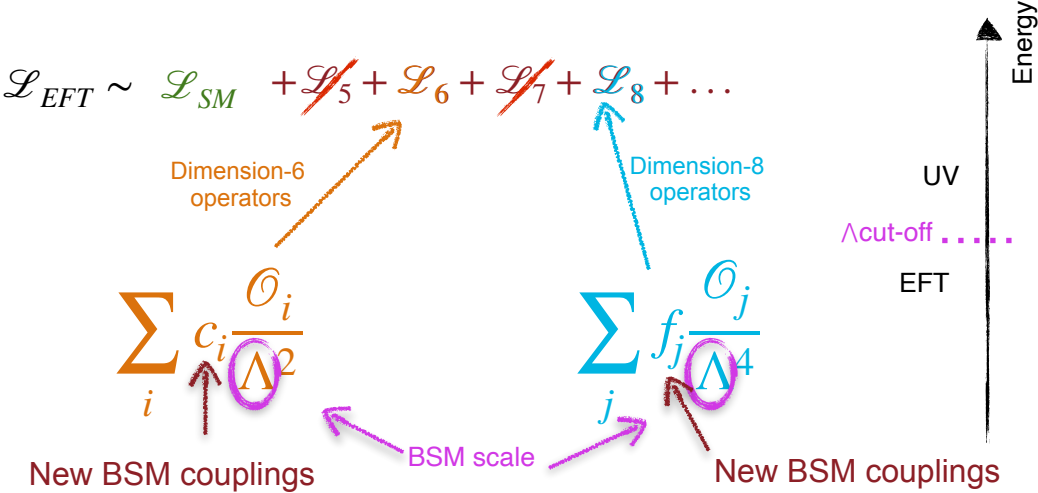
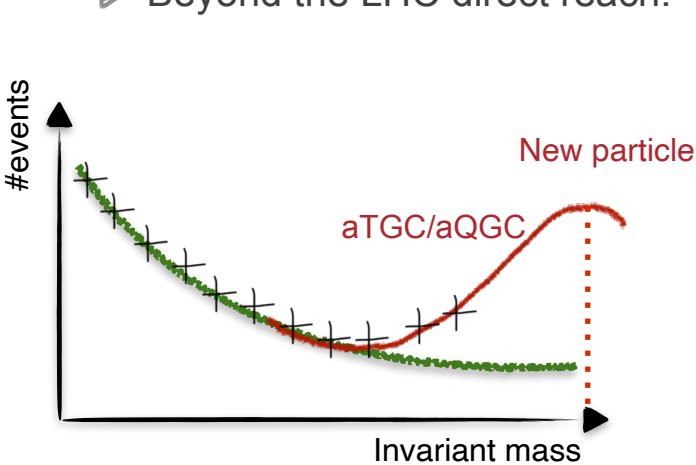


Contact interactions



The EFT framework

- ▶ Parametrize deviations from the SM in terms of an Effective Field Theory (EFT)
 - ▶ Beyond the LHC direct reach!



▶ In the past: Diboson for dim6 & VBS for dim8



Vector
Boson
Scattering

muon

electron

VBS jet

VBS jet

electron

muon

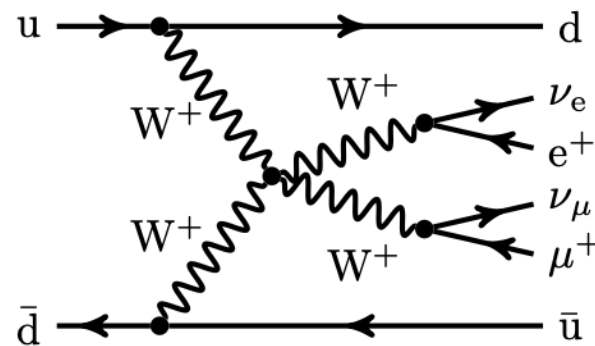
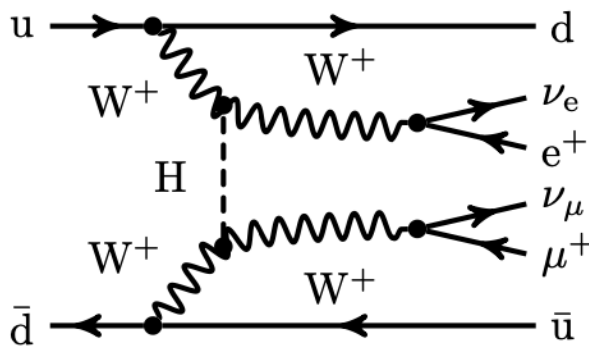
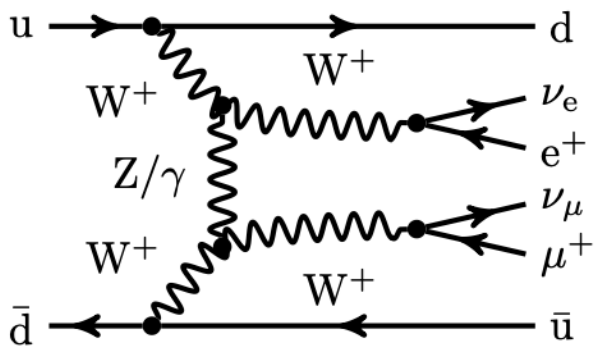
Vector Boson Scattering

- Three contributions at LO:

1. Pure EWK $O(\alpha_{EW}^6)$ → signal

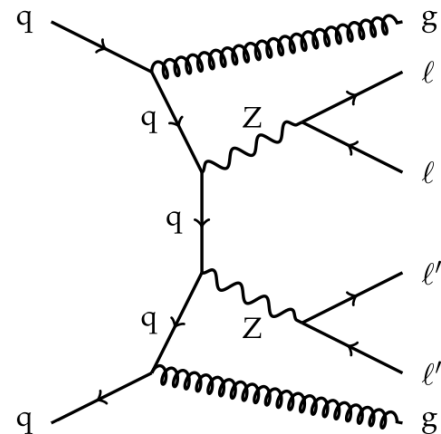
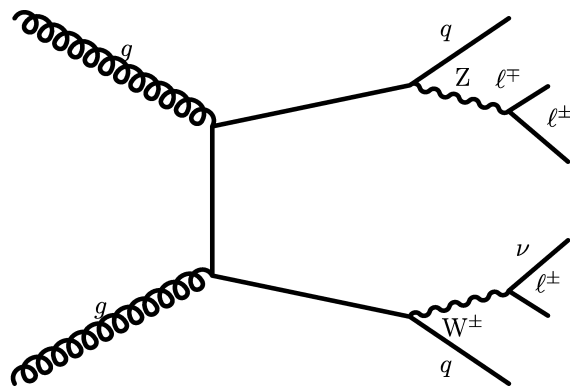
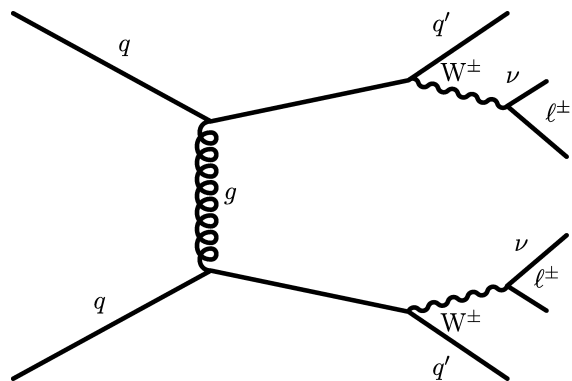
2. QCD-induced $O(\alpha_{EW}^4 \alpha_S^2)$ - irreducible contribution

3. EWK-QCD interference $O(\alpha_{EW}^5 \alpha_S)$

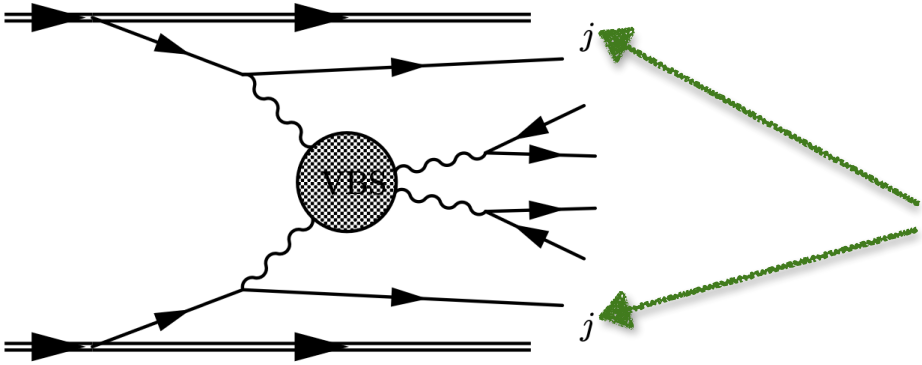


Vector Boson Scattering

- Three contributions at LO:
 1. Pure EWK $O(\alpha_{EW}^6)$ \rightarrow signal
 2. **QCD-induced $O(\alpha_{EW}^4 \alpha_S^2)$ - irreducible contribution**
 3. **EWK-QCD interference $O(\alpha_{EW}^5 \alpha_S)$**



VBS signal



- ▶ **VBS jets:** Two very energetic forward-backward QUARK-initiated jets
 - ▶ Large m_{jj} and $\Delta\eta_{jj}$

3 signatures depending on the decay of the vector bosons:

Fully leptonic:
Pure but low BR

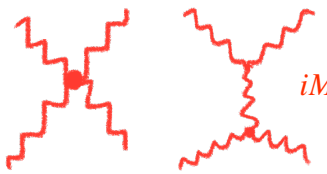
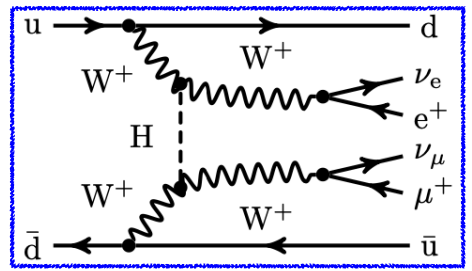
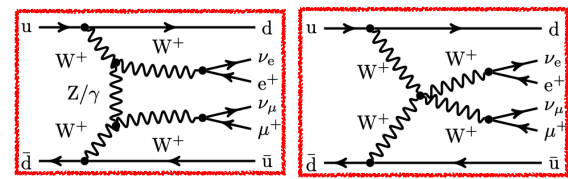
Semi-leptonic:
Balance purity & BR

Fully hadronic: High BR & access
to high energy tails but high bkg,
Run2 results are yet to come!

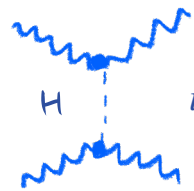
Main backgrounds: $t\bar{t}$ /top, DY, non-prompt leptons, diboson

why VBS processes?

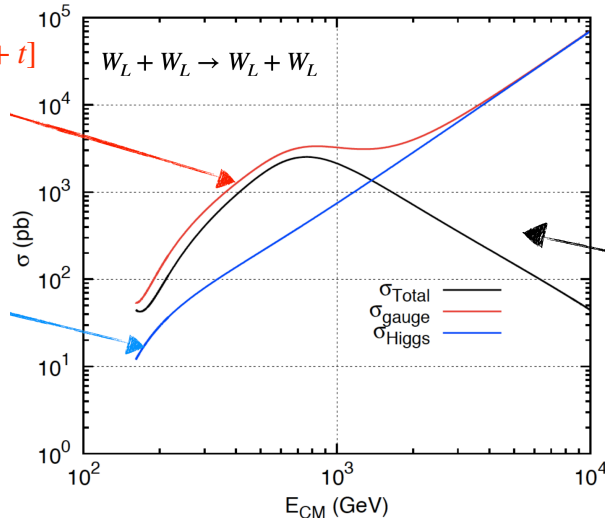
- Probes two key aspects of the SM together
 - Gauge interactions: triple and quartic gauge couplings
 - Couplings between the Higgs and the gauge bosons
 - complementary to direct measurements



$$iM_{gauge} \simeq -i \frac{g^2}{4m_W^2} [s + t]$$



$$iM_{Higgs} \simeq i \frac{g^2}{4m_W^2} [s + t]$$



cancels exactly the E^2 dependence of the cross section at high energy

VBS Run2 results:

First evidence and observations for rare processes

Fully leptonic

Semi-leptonic

NEW

Forward protons and hadronic V

PROCESS	LUMI [fb ⁻¹]	RESULTS	REFERENCE
VBS in ssWW + WZ	Full Run 2 (137/fb)	Observation & XS + dim-8 EFT limits	PLB 809 (2020) 135710
polarized VBS ssWW	Full Run 2 (137/fb)	W _L W _L measurement	PLB 812 (2020) 136018
VBS ZZ	Full Run 2 (137/fb)	Evidence + dim-8	PLB 812 (2021) 135992
VBS osWW	Full Run 2 (137/fb)	Observation & XS	arXiv:2205.05711 , sub. PLB
VBS WV	Full Run 2 (137/fb)	Evidence	PLB 834 (2022) 137438
VBS WV/ZV	2016 data (36/fb)	Dim-8 EFT limits	PLB 798 (2019)134985
VBS ssWW with taus	Full Run 2 (137/fb)	2.7 σ	CMS-SMP-22-008
VBS W γ	Full Run 2 (137/fb)	Observation, differential XS + dim-8 EFT limits	PLB 811 (2020) 135988 arXiv:2212.12592 , acc. PRD
VBS Z γ	Full Run 2 (137/fb)	Observation, differential XS + dim-8 EFT limits	PRD 104 (2021) 072001
VBS PPS $\gamma\gamma$ VV	Full Run 2 PPS (100/fb)	Dim-6 and dim-8	arXiv:2211.16320 , acc. JHEP

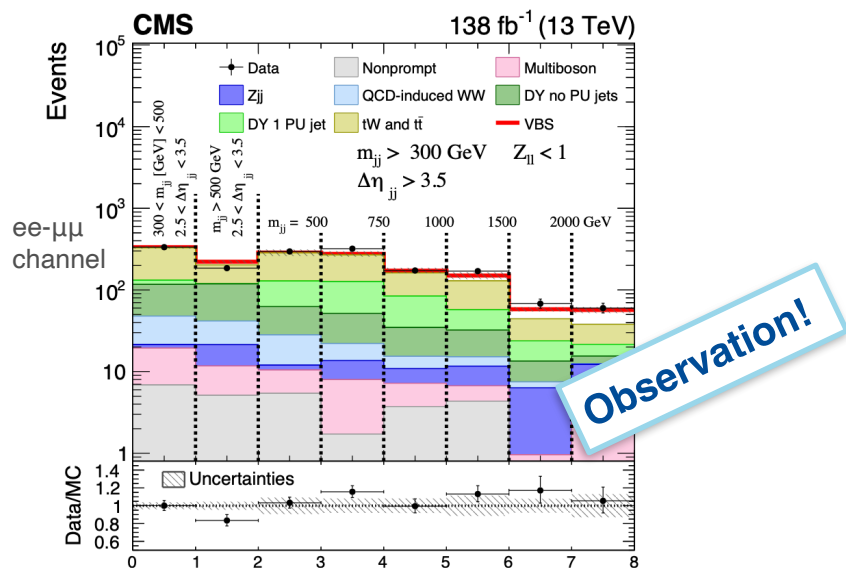
Stringent limits on EFT coefficients



Highlights on “Firsts”:

► VBS osWW [[arXiv:2205.05711](https://arxiv.org/abs/2205.05711)]

- Obs. (exp.) significance 5.6 (5.2)
- Fiducial cross-sections:
 10.2 ± 2.0 fb (theory: 9.1 ± 0.6 fb)

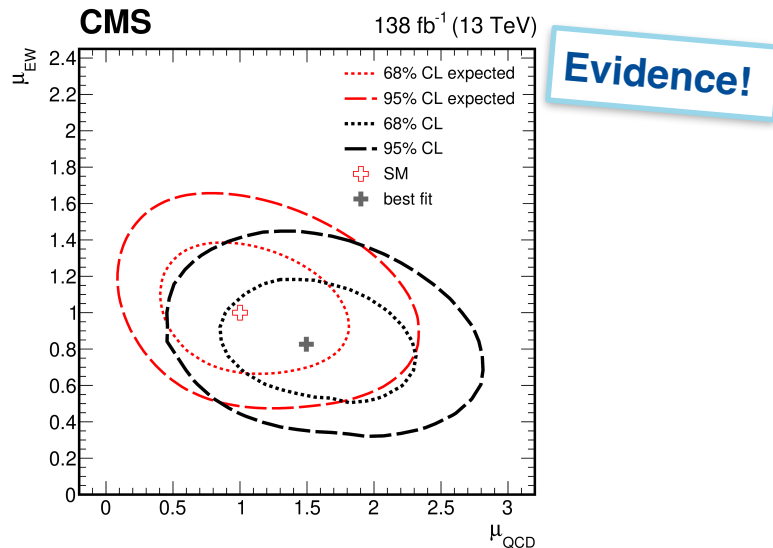


$$Z_{\ell\ell} = \frac{1}{2} |Z_{\ell_1} + Z_{\ell_2}|, \quad \text{where } Z_{\ell_i} = \eta_{\ell_i} - \frac{1}{2}(\eta_{j_1} + \eta_{j_2})$$

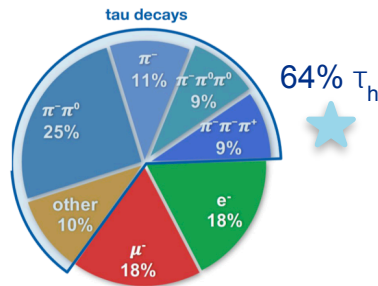
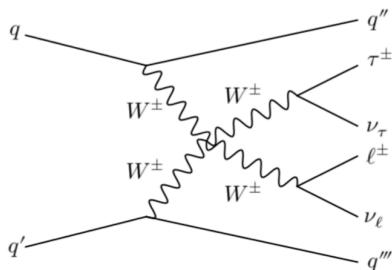
► VBS WW semileptonic

[[PLB 834 \(2022\) 137438](https://arxiv.org/abs/2205.05711)]

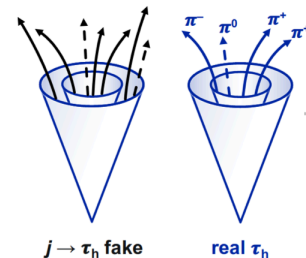
- Evidence obs. (exp.) significance 4.4 (5.1)
- EW_{WW} xsec obs. (exp.) $1.90^{+0.53}_{-0.46}$ pb (2.23)
- $\mu_{\text{EW}} = 0.85 \pm 0.12$ (stat) $^{+0.19}_{-0.17}$ (syst)



New:



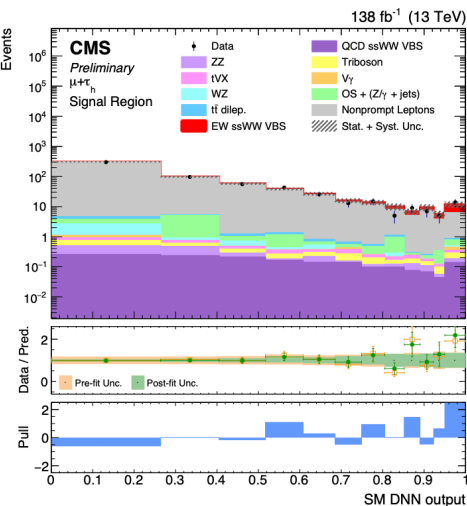
Tau decay for the first time in VBS ssWW!



VBS ssWW with τ_h

[CMS-SMP-22-008]

- ▶ Main background nonprompt leptons from jets misreconstructed as e, μ , or τ_h
 - ▶ estimated from data, and validated in a CR
 - ▶ Uncertainty is statistically dominated



- VBS jet pair invariant mass M_{jj} ;
- transverse mass $M_T(\ell, \vec{p}_T^{\text{miss}})$;
- transverse mass M_{1T} ;
- transverse mass M_{01} ;
- p_T of leading VBS jet;
- p_T of subleading VBS jet;
- p_T of τ_h ;
- p_T of ℓ ;
- ratio of p_T of the leading track of the jet associated with τ_h to the $\tau_h p_T$.

$$M_{1T}^2 = \left(\sqrt{M_{\ell\ell}^2 + p_T^{\ell 2}} + p_T^{\text{miss}} \right)^2 - \left| \vec{p}_T^{\ell} + \vec{p}_T^{\text{miss}} \right|^2,$$

$$M_{01}^2 = \left(p_T^{\tau} + p_T^{\ell} + p_T^{\text{miss}} \right)^2 - \left| \vec{p}_T^{\tau} + \vec{p}_T^{\ell} + \vec{p}_T^{\text{miss}} \right|^2.$$

Signal	Significance $[\sigma]$	
	Expected	Observed
pure EW ssWW VBS	1.94	2.74
EW + QCD ssWW VBS	2.04	2.87

★ τ high mass → preferential coupling to the Higgs



Highlights on firsts:

► VBS fully leptonic

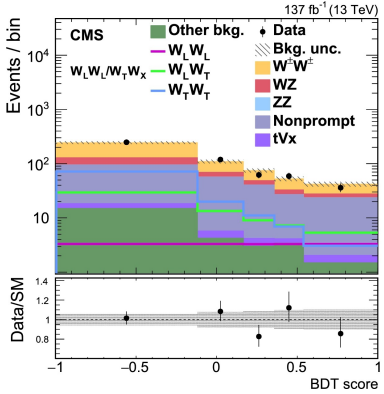
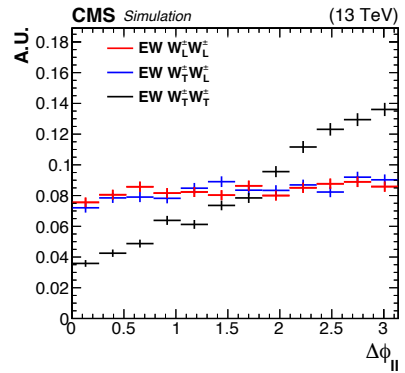
- Differential ssWW xsec measurement + observation of VBS WZ

Obs. (exp.) significance 6.8(5.3)

[[PLB 809 \(2020\) 135710](#)]

► Polarization in ssWW [[PLB 812 \(2020\) 136018](#)]

- obs. (exp.) xsec for $W_L^\pm W_L^\pm$: 1.17 (0.88) fb (in WW RF)
- obs. (exp.) significance for $W_L^\pm W_X^\pm$: 2.3 (3.1)



► VBS PPS $\gamma\gamma WW/ZZ$ [[arXiv:2211.16320](#)] (CMS+TOTEM)

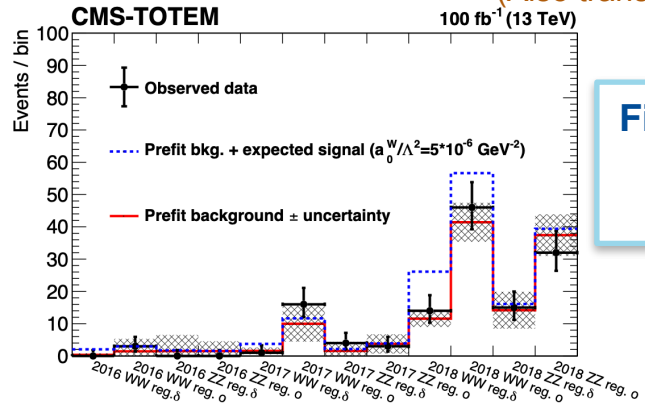
- Upper limits on pp → pWWp / pZZp cross sections
- aQGC limits w/o “clipping” for unitarity

Coupling	Observed (expected) 95% CL upper limit No clipping	Observed (expected) 95% CL upper limit Clipping at 1.4 TeV
$ a_0^W / \Lambda^2 $	4.3 (3.9) × 10 ⁻⁶ GeV ⁻²	5.2 (5.1) × 10 ⁻⁶ GeV ⁻²
$ a_C^W / \Lambda^2 $	1.6 (1.4) × 10 ⁻⁵ GeV ⁻²	2.0 (2.0) × 10 ⁻⁵ GeV ⁻²
$ a_0^Z / \Lambda^2 $	0.9 (1.0) × 10 ⁻⁵ GeV ⁻²	—
$ a_C^Z / \Lambda^2 $	4.0 (4.5) × 10 ⁻⁵ GeV ⁻²	—

~ 15-20 times better than Run1

Dim6

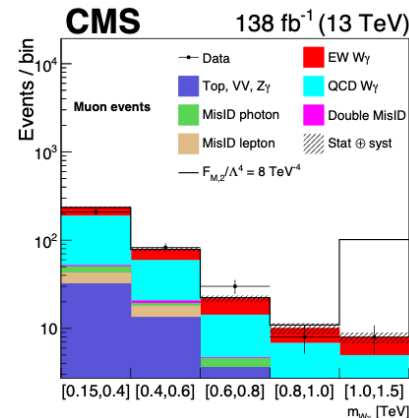
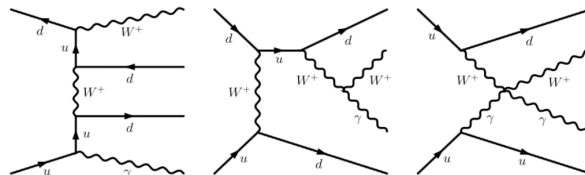
(Also translated to dim8)



First limits on aQGC in $\gamma\gamma \rightarrow ZZ$

VBS W_γ

- Final states: $e\nu\gamma + 2\text{jets}$ and $\mu\nu\gamma + 2\text{jets}$
- Data-driven background estimate:
 - Template fit: non-prompt photon
 - Tight-loose method: non-prompt lepton
- Fiducial and differential cross section
- Probes quadratic and triple gauge couplings
- Limits setting on EFT dim-8 operators



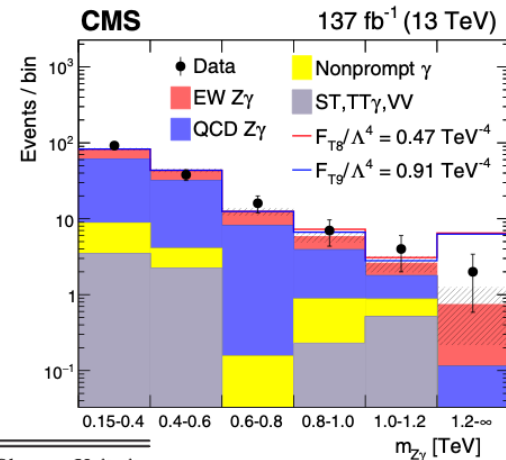
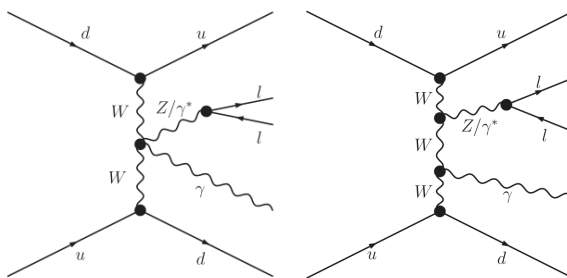
- Limits obtained varying the coefficient of one operator at a time
 - all others set to zero (SM value).
- Unitary bound: scattering energy at which the aQGC coupling strength, when set equal to the observed limit, would result in a scattering amplitude that violates unitarity.

Expected limit	Observed limit	U_{bound}
$-5.1 < f_{M,0}/\Lambda^4 < 5.1$	$-5.6 < f_{M,0}/\Lambda^4 < 5.5$	1.7
$-7.1 < f_{M,1}/\Lambda^4 < 7.4$	$-7.8 < f_{M,1}/\Lambda^4 < 8.1$	2.1
$-1.8 < f_{M,2}/\Lambda^4 < 1.8$	$-1.9 < f_{M,2}/\Lambda^4 < 1.9$	2.0
$-2.5 < f_{M,3}/\Lambda^4 < 2.5$	$-2.7 < f_{M,3}/\Lambda^4 < 2.7$	2.7
$-3.3 < f_{M,4}/\Lambda^4 < 3.3$	$-3.7 < f_{M,4}/\Lambda^4 < 3.6$	2.3
$-3.4 < f_{M,5}/\Lambda^4 < 3.6$	$-3.9 < f_{M,5}/\Lambda^4 < 3.9$	2.7
$-13 < f_{M,7}/\Lambda^4 < 13$	$-14 < f_{M,7}/\Lambda^4 < 14$	2.2
$-0.43 < f_{T,0}/\Lambda^4 < 0.51$	$-0.47 < f_{T,0}/\Lambda^4 < 0.51$	1.9
$-0.27 < f_{T,1}/\Lambda^4 < 0.31$	$-0.31 < f_{T,1}/\Lambda^4 < 0.34$	2.5
$-0.72 < f_{T,2}/\Lambda^4 < 0.92$	$-0.85 < f_{T,2}/\Lambda^4 < 1.0$	2.3
$-0.29 < f_{T,5}/\Lambda^4 < 0.31$	$-0.31 < f_{T,5}/\Lambda^4 < 0.33$	2.6
$-0.23 < f_{T,6}/\Lambda^4 < 0.25$	$-0.25 < f_{T,6}/\Lambda^4 < 0.27$	2.9
$-0.60 < f_{T,7}/\Lambda^4 < 0.68$	$-0.67 < f_{T,7}/\Lambda^4 < 0.73$	3.1

Most
stringent

VBS $Z\gamma$

- Final states: $\ell^+\ell^-\gamma + 2\text{jets}$ with $\ell = e, \mu$
- Main background QCD-induced $Z\gamma jj$, from simulation, constrained in data
- Z +jets with selected photon not prompt, data-driven



- Obs. (exp.) significance 9.4 (8.5)
- Fiducial EW cross-sections:
 5.21 ± 0.52 (stat) ± 0.56 (syst) fb
- Provide several unfolded differential xsecs

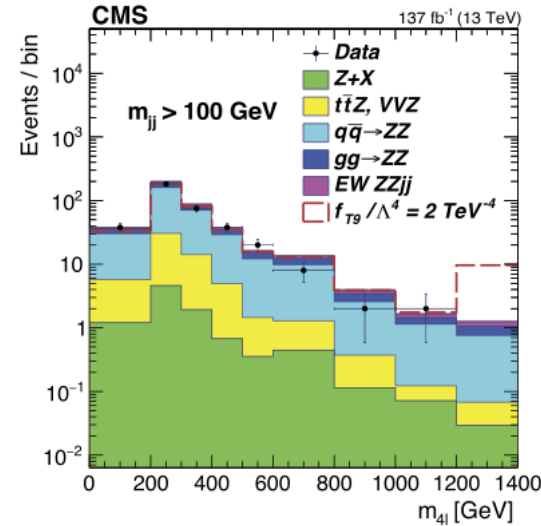
- Uncertainty is statistically dominated

Coupling	Exp. lower	Exp. upper	Obs. lower	Obs. upper	Unitarity bound
F_{M0}/Λ^4	-12.5	12.8	-15.8	16.0	1.3
F_{M1}/Λ^4	-28.1	27.0	-35.0	34.7	1.5
F_{M2}/Λ^4	-5.21	5.12	-6.55	6.49	1.5
F_{M3}/Λ^4	-10.2	10.3	-13.0	13.0	1.8
F_{M4}/Λ^4	-10.2	10.2	-13.0	12.7	1.7
F_{M5}/Λ^4	-17.6	16.8	-22.2	21.3	1.7
F_{M7}/Λ^4	-44.7	45.0	-56.6	55.9	1.6
F_{T0}/Λ^4	-0.52	0.44	-0.64	0.57	1.9
F_{T1}/Λ^4	-0.65	0.63	-0.81	0.90	2.0
F_{T2}/Λ^4	-1.36	1.21	-1.68	1.54	1.9
F_{T5}/Λ^4	-0.45	0.52	-0.58	0.64	2.2
F_{T6}/Λ^4	-1.02	1.07	-1.30	1.33	2.0
F_{T7}/Λ^4	-1.67	1.97	-2.15	2.43	2.2
F_{T8}/Λ^4	-0.36	0.36	-0.47	0.47	1.8
F_{T9}/Λ^4	-0.72	0.72	-0.91	0.91	1.9

Most
stringent

- Main background: production of 2Z bosons + QCD-induced jets, from simulation, constrained in data
- Other irreducible backgrounds: processes with high-pT isolated leptons $t\bar{t}Z$ +jets and VVZ +jets, from simulation
- Reducible backgrounds: heavy-flavor jets produce secondary leptons or jets misidentified as leptons as Z +jets, $t\bar{t}$ +jets and WZ +jets
- Main uncertainty on X sec measurements: QCD renormalization and factorization scales (signal) and jet energy scale $\sim 10\%$

- ▶ Two approaches, the distributions of the SM processes, including the EW component, are normalized
 - 1) to their measured values in the EW signal extraction
 - 2) to their expected values.
- ▶ Uncertainty is statistically dominated

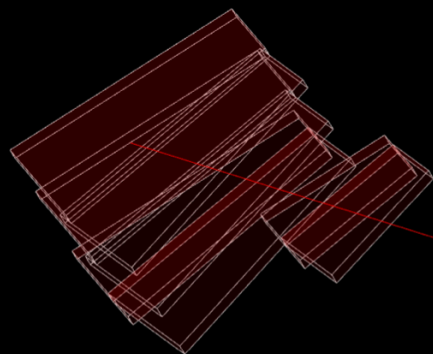


Coupling	Exp. lower	Exp. upper	Obs. lower	Obs. upper	Unitarity bound
f_{T0}/Λ^4	-0.37	0.35	-0.24 (-0.26)	0.22 (0.24)	2.4
f_{T1}/Λ^4	-0.49	0.49	-0.31 (-0.34)	0.31 (0.34)	2.6
f_{T2}/Λ^4	-0.98	0.95	-0.63 (-0.69)	0.59 (0.65)	2.5
f_{T8}/Λ^4	-0.68	0.68	-0.43 (-0.47)	0.43 (0.48)	1.8
f_{T9}/Λ^4	-1.5	1.5	-0.92 (-1.02)	0.92 (1.02)	1.8

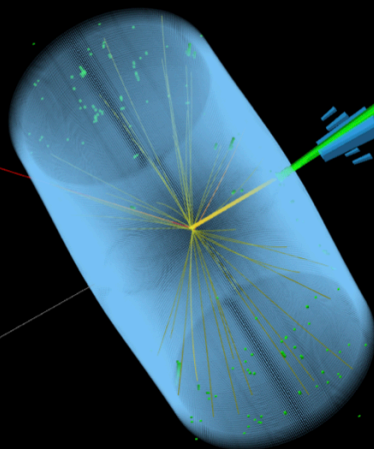
Most stringent



$W \rightarrow \mu \nu$



$\mu p_T > 240 \text{ GeV}$



$\gamma E_T > 530 \text{ GeV}$

Missing $p_T > 290 \text{ GeV}$

DIBOSON

Diboson Run2 results:

Interference resurrection

PROCESS	LUMI [fb ⁻¹]	RESULTS	REFERENCE
WZ	Full Run 2 (137/fb)	Differential XS + aTGC limits	JHEP 07 (2022) 032
WW, WZ, ZZ	2017 (302/pb) 5.02 TeV	EWK XS	PRL 127 (2021) 191801
ZZ	Full Run 2 (137/fb)	XS + aTGC limits	EPJC 81 (2021) 200
osWW	2016 (35.9/fb)	XS + dim6 limits	PRD 102 (2020) 092001
W γ	Full Run 2 (138/fb)	differential XS + dim-6 EFT limits	PRD 105 (2022) 052003 PRL 126 (2021) 252002

Stringent limits on EFT coefficients

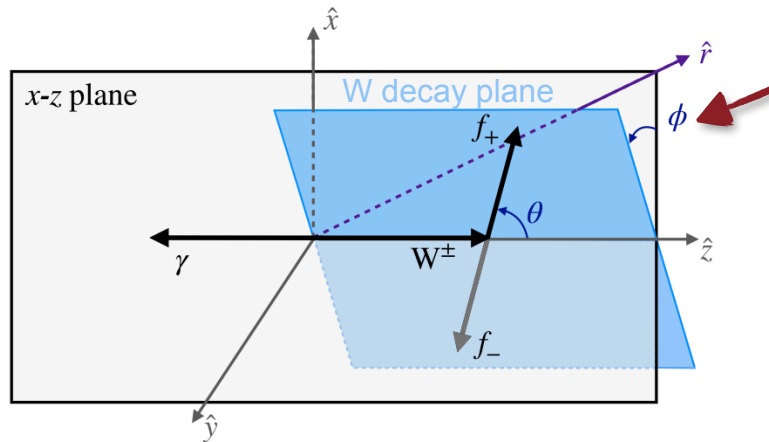
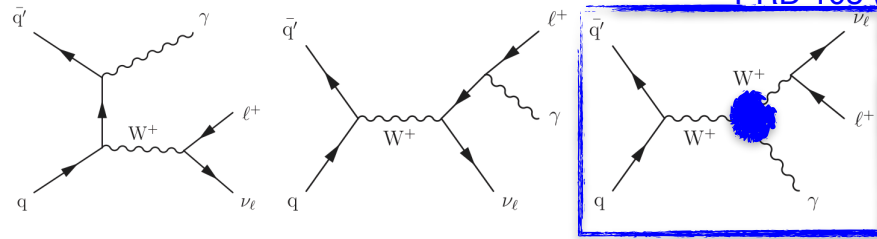
W γ : interference resurrection

► Dim6 O_{3W} CP-even modification of the WWV TGC

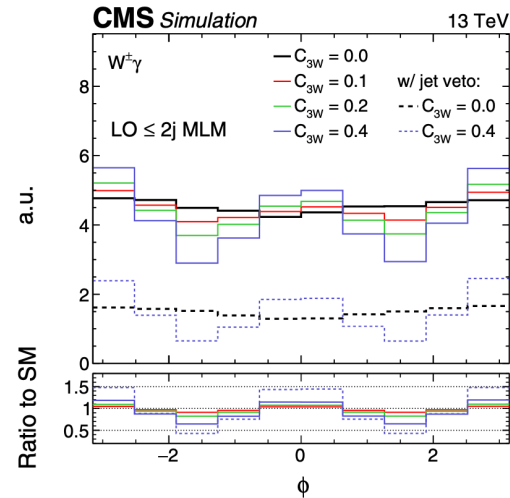
$$\sigma(C_{3W}) = \sigma^{\text{SM}} + C_{3W} \sigma^{\text{int}} + C_{3W}^2 \sigma^{\text{BSM}}$$

Wilson Coefficient

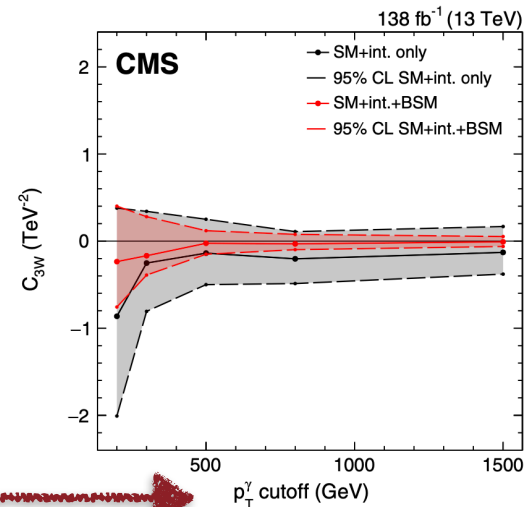
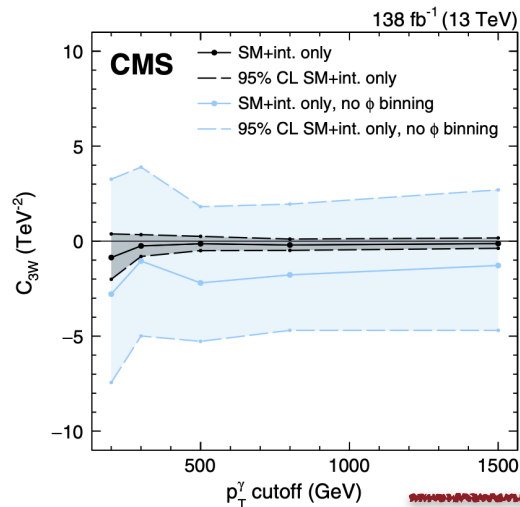
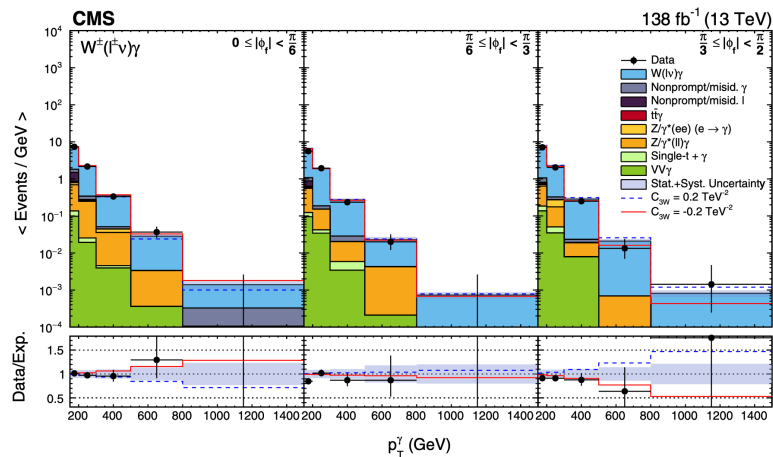
Interference term ($\sim \Lambda^{-2}$) \rightarrow not accessible with variables inclusive over the decay angles



- coordinate system: Lorentz boost to the center-of-mass frame of the W γ system



W_γ : interference resurrection



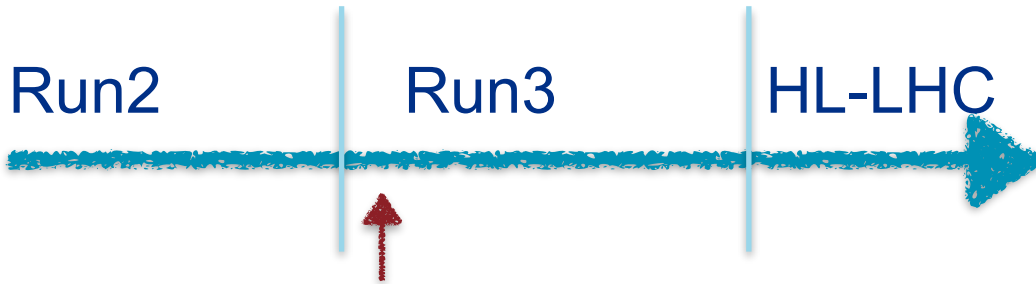
Factor 10 improvement using the ϕ binning

► Prefit: good background modeling

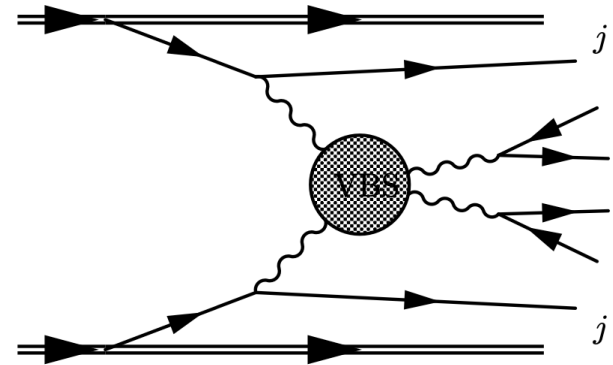
p_T^γ cutoff (GeV)	Best fit C_{3W} (TeV^{-2})		Observed 95% CL (TeV^{-2})		Expected 95% CL (TeV^{-2})	
	SM + int. only	SM + int. + BSM	SM + int. only	SM + int. + BSM	SM + int. only	SM + int. + BSM
200	-0.86	-0.24	[-2.01, 0.38]	[-0.76, 0.40]	[-1.16, 1.27]	[-0.81, 0.71]
300	-0.25	-0.17	[-0.81, 0.34]	[-0.39, 0.28]	[-0.56, 0.60]	[-0.33, 0.33]
500	-0.13	-0.025	[-0.50, 0.25]	[-0.15, 0.12]	[-0.35, 0.38]	[-0.17, 0.16]
800	-0.20	-0.033	[-0.49, 0.11]	[-0.10, 0.08]	[-0.29, 0.31]	[-0.097, 0.095]
1500	-0.13	-0.009	[-0.38, 0.17]	[-0.062, 0.052]	[-0.27, 0.29]	[-0.066, 0.065]

► For interpretations with highest bins beyond the validity of the EFT or specific BSM model

Multiboson results* in CMS



Run2 is wrapping up
but is too early for
Run3 results



*and some(!) ideas 

Jet tagging

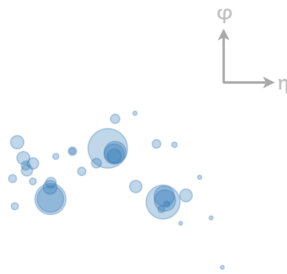
ML taggers are improving the identification performance

- ▶ B-tagging to reduce $t\bar{t}$ background
- ▶ (Boosted) W/Z tagging
- ▶ q/g discrimination

Could be applied to other tasks

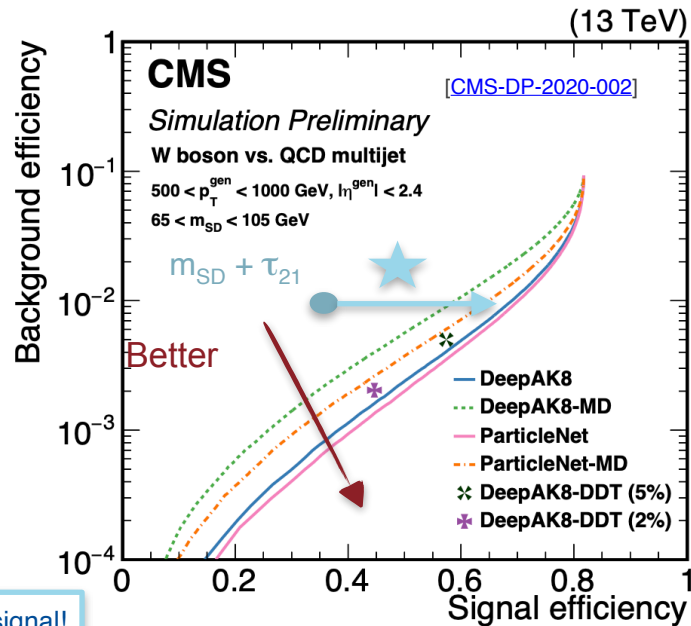
One example: ParticleNet [PRD 101 (2020) 056019]

- Graph NN with jets as an unordered set of particles



■ Particle cloud

- particles are intrinsically *unordered*
- primary information:
 - 2D coordinates in the η - ϕ space
 - Plus all other particle properties as momentum, charge, etc.



50% more signal!

Jet tagging

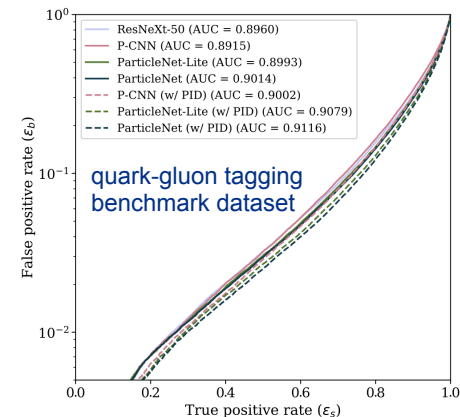
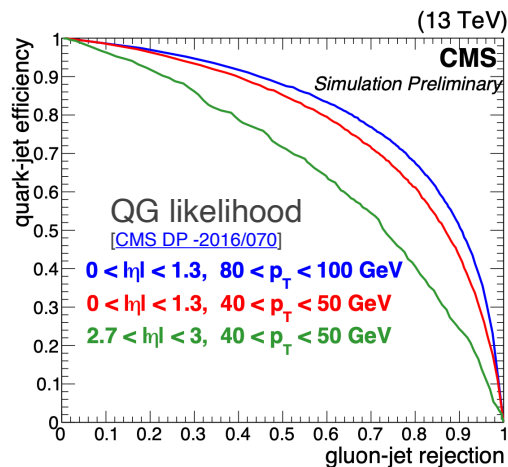
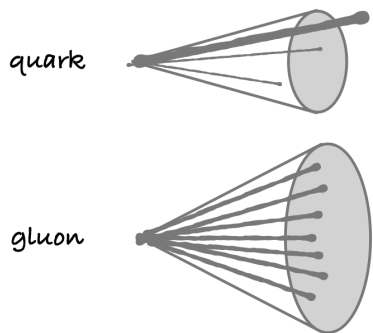
ML taggers are improving the identification performance

- ▶ B-tagging to reduce $t\bar{t}$ background
- ▶ (Boosted) W/Z tagging
- ▶ q/g discrimination

Could be applied to other tasks

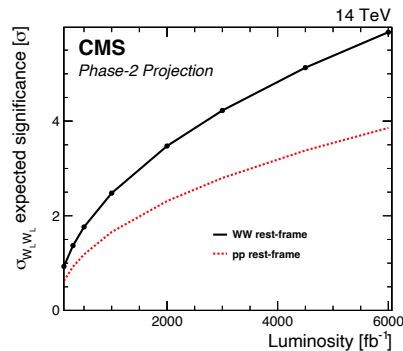
One example: ParticleNet [[PRD 101 \(2020\) 056019](#)]

- Graph NN with jets as an unordered set of particles



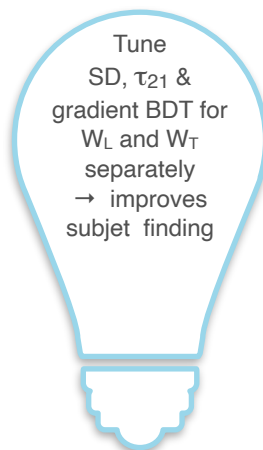
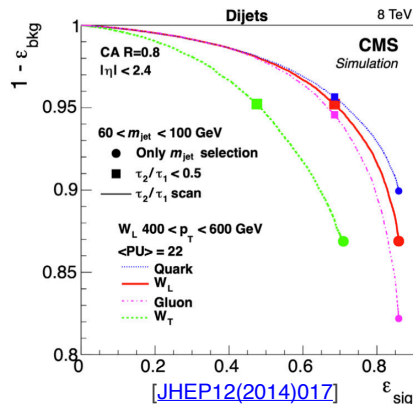
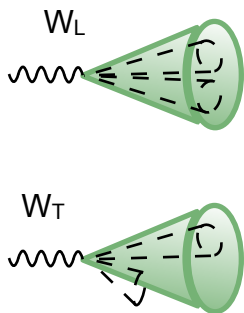
Polarization

- Challenging measurement: $V_L V_L \rightarrow V_L V_L$ is $\sim 10\%$ of the total EW WW scattering cross section
 - Still! Significance of ~ 1 (3) standard deviations for WLWL (WLWX) in Run2 [PLB 812 (2020) 136018]
 - Extrapolating it the prediction at HL-LHC are improved wrt previous estimates
 - use of more sophisticated techniques to discriminate between signal and backgrounds

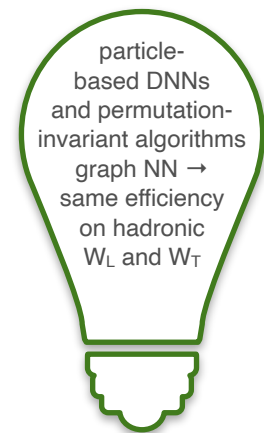


- Can we improve the sensitivity? Can we use other channels?

(Boosted) hadronic channel has info on all final state objects! \rightarrow but improvements are needed



[arXiv:2110.02773v2]

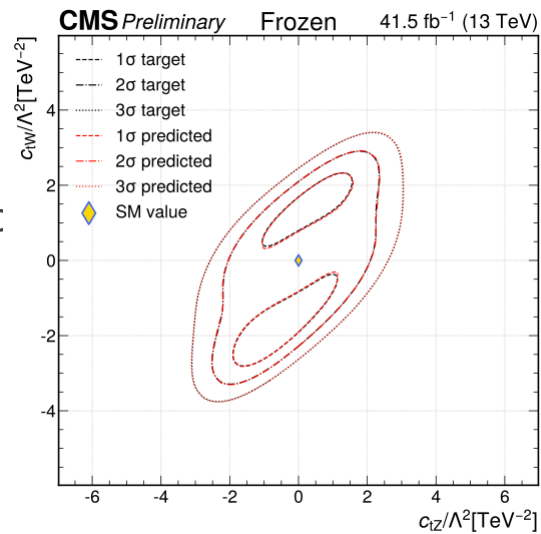


JEDI-Net [arXiv:1908.05318]
ParticleNet [PRD 101 (2020) 056019]

More details?

- ▶ Run1 & Run2:
 - ▶ Observe SM rare processes
 - ▶ First EFT limits
 - ▶ Obtained varying the coefficient of one operator at a time (all others set to zero - SM value).
- ▶ **IF** we see something, we need to characterize it
- ▶ Can we better describe the correlations among operators?
- ▶ [[CMS DP -2023/027](#)] uses a DNN to approximate the profiled ΔNLL with high accuracy
 - ▶ Samples ~ 50 million points across the 16D Wilson coefficient space with the nuisances profiled away in the process
 - ▶ Regions with high likelihood are more heavily sampled to enhance DNN performance in these regions of interest.
 - ▶ Validated reproducing published 1D & 2D scans
 - ▶ Can be used also for reparametrizations in WC space

Do we see something?



Summary



CMS Experiment at the LHC, CERN

Data recorded: 2016-Jul-08 23:47:39.259242 GMT

Run / Event / LS: 276525 / 2665335317 / 1561

Real VBS event

- Run2 is wrapping up:
 - First polarization
 - Some channels are still uncovered
 - Explored interference resurrection
 - Limit setting w/ clipping & unitary bound
 - And as a function of the cutoff
- New opportunities to get the most of Run3 & HL-LHC

muon

electron

VBS jet

VBS jet

electron

muon

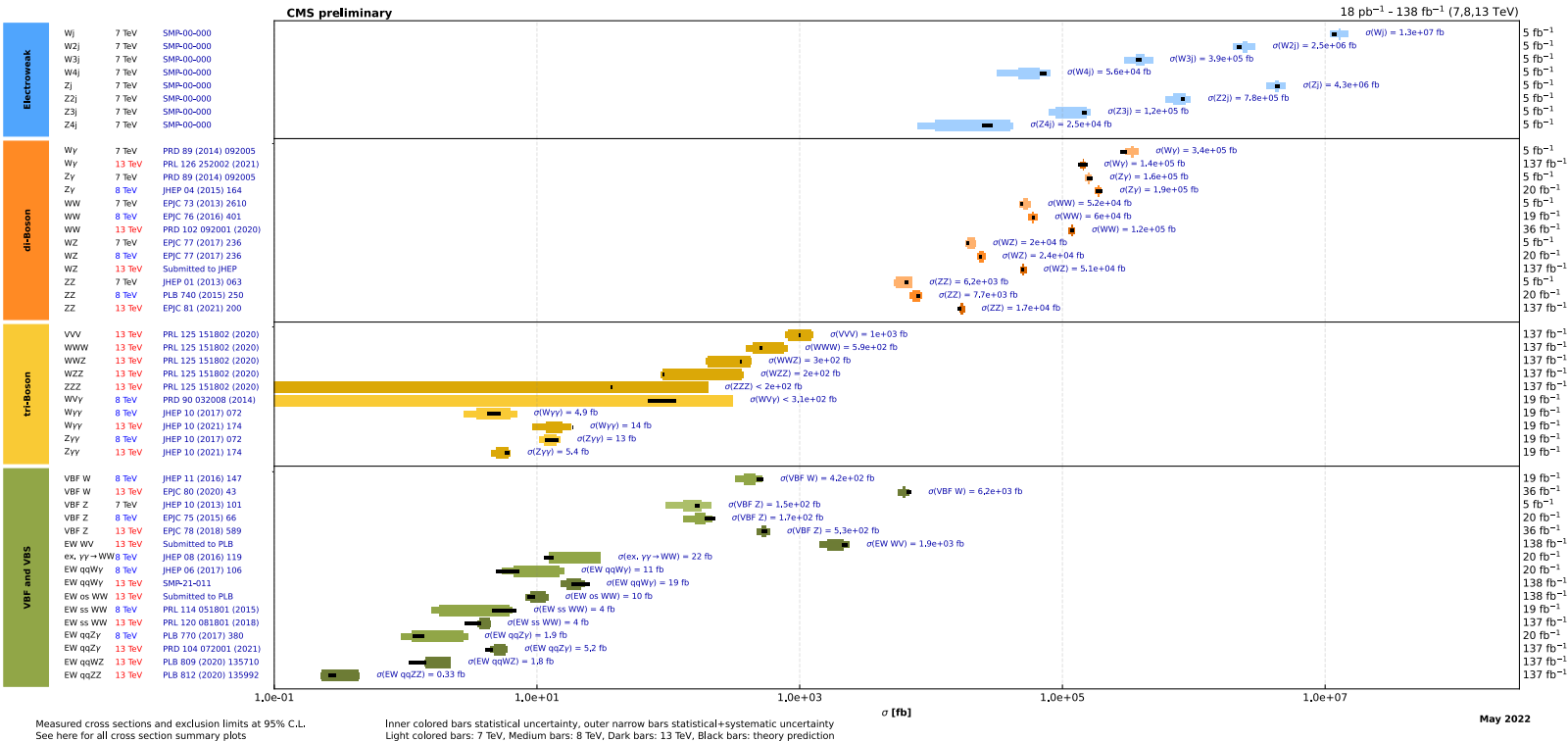
More to come!!

Thanks!

Many inputs from the Report from Standard Model Physics
Analysis Group at Physics Days: Effective Field Theory
Saptaparna Bhattacharya, Giacomo Boldrini, Andrew Gilbert,
Pietro Govoni

Additional material

Overview of CMS cross section results



Full slew of Effective Field Theory operators at dimension-6

$\mathcal{L}_6^{(1)} - X^3$		$\mathcal{L}_6^{(6)} - \psi^2 XH$		$\mathcal{L}_6^{(8b)} - (\bar{R}R)(\bar{R}R)$	
Q_G	$f^{abc} G_{\mu\nu}^a G_{\nu\rho}^b G_{\rho\mu}^c$	Q_{eW}	$(\bar{l}_p \sigma^{\mu\nu} e_r) \sigma^4 H W_{\mu\nu}^1$	Q_{ee}	$(\bar{e}_p \gamma_\mu e_r) (\bar{e}_s \gamma^\mu e_t)$
$Q_{\bar{G}}$	$f^{abc} \bar{G}_{\mu\nu}^a G_{\nu\rho}^b G_{\rho\mu}^c$	Q_{eB}	$(\bar{l}_p \sigma^{\mu\nu} e_r) H B_{\mu\nu}$	Q_{uu}	$(\bar{u}_p \gamma_\mu u_r) (\bar{u}_s \gamma^\mu u_t)$
Q_W	$\varepsilon^{ijk} W_{\mu\nu}^i W_{\nu\rho}^j W_{\rho\mu}^k$	Q_{uG}	$(\bar{q}_p \sigma^{\mu\nu} T^a u_r) \bar{H} G_{\mu\nu}^a$	Q_{dd}	$(\bar{d}_p \gamma_\mu d_r) (\bar{d}_s \gamma^\mu d_t)$
$Q_{\bar{W}}$	$\varepsilon^{ijk} \bar{W}_{\mu\nu}^i W_{\nu\rho}^j W_{\rho\mu}^k$	Q_{uW}	$(\bar{q}_p \sigma^{\mu\nu} u_r) \sigma^4 \bar{H} W_{\mu\nu}^1$	Q_{eu}	$(\bar{e}_p \gamma_\mu e_r) (\bar{u}_s \gamma^\mu u_t)$
	$\mathcal{L}_6^{(2)} - H^6$	Q_{uB}	$(\bar{q}_p \sigma^{\mu\nu} u_r) \bar{H} B_{\mu\nu}$	Q_{ed}	$(\bar{e}_p \gamma_\mu e_r) (\bar{d}_s \gamma^\mu d_t)$
Q_H	$(H^\dagger H)^3$	Q_{dG}	$(\bar{q}_p \sigma^{\mu\nu} T^a d_r) H G_{\mu\nu}^a$	$Q_{ud}^{(1)}$	$(\bar{u}_p \gamma_\mu u_r) (\bar{d}_s \gamma^\mu d_t)$
	$\mathcal{L}_6^{(3)} - H^4 D^2$	Q_{dW}	$(\bar{q}_p \sigma^{\mu\nu} d_r) \sigma^4 H W_{\mu\nu}^1$	$Q_{ud}^{(8)}$	$(\bar{u}_p \gamma_\mu T^a u_r) (\bar{d}_s \gamma^\mu T^a d_t)$
$Q_{H\Box}$	$(H^\dagger H) \Box (H^\dagger H)$	Q_{dB}	$(\bar{q}_p \sigma^{\mu\nu} d_r) H B_{\mu\nu}$		
Q_{HD}	$(D^\mu H^\dagger H) (H^\dagger D_\mu H)$				
$\mathcal{L}_6^{(4)} - X^2 H^2$		$\mathcal{L}_6^{(7)} - \psi^2 H^2 D$		$\mathcal{L}_6^{(8c)} - (\bar{L}L)(\bar{R}R)$	
Q_{HG}	$H^\dagger H G_{\mu\nu}^a G^{a\mu\nu}$	$Q_{H\Box}^{(1)}$	$(H^\dagger i \overleftrightarrow{D}_\mu H) (\bar{l}_p \gamma^\mu l_r)$	Q_{le}	$(\bar{l}_p \gamma_\mu l_r) (\bar{e}_s \gamma^\mu e_t)$
$Q_{H\bar{G}}$	$H^\dagger H \bar{G}_{\mu\nu}^a G^{a\mu\nu}$	$Q_{H\Box}^{(3)}$	$(H^\dagger i \overleftrightarrow{D}_\mu^2 H) (\bar{l}_p \sigma^i \gamma^\mu l_r)$	Q_{lu}	$(\bar{l}_p \gamma_\mu l_r) (\bar{u}_s \gamma^\mu u_t)$
Q_{HW}	$H^\dagger H W_{\mu\nu}^1 W^{1\mu\nu}$	Q_{He}	$(H^\dagger i \overleftrightarrow{D}_\mu H) (\bar{e}_p \gamma^\mu e_r)$	Q_{ld}	$(\bar{l}_p \gamma_\mu l_r) (\bar{d}_s \gamma^\mu d_t)$
$Q_{H\bar{W}}$	$H^\dagger H \bar{W}_{\mu\nu}^1 W^{1\mu\nu}$	$Q_{Hq}^{(1)}$	$(H^\dagger i \overleftrightarrow{D}_\mu H) (\bar{q}_p \gamma^\mu q_r)$	Q_{qe}	$(\bar{q}_p \gamma_\mu q_r) (\bar{e}_s \gamma^\mu e_t)$
Q_{HB}	$H^\dagger H B_{\mu\nu} B^{\mu\nu}$	$Q_{Hq}^{(3)}$	$(H^\dagger i \overleftrightarrow{D}_\mu^2 H) (\bar{q}_p \sigma^i \gamma^\mu q_r)$	$Q_{qu}^{(1)}$	$(\bar{q}_p \gamma_\mu q_r) (\bar{u}_s \gamma^\mu u_t)$
$Q_{H\bar{B}}$	$H^\dagger H \bar{B}_{\mu\nu} B^{\mu\nu}$	Q_{Hu}	$(H^\dagger i \overleftrightarrow{D}_\mu H) (\bar{u}_p \gamma^\mu u_r)$	$Q_{qu}^{(8)}$	$(\bar{q}_p \gamma_\mu T^a q_r) (\bar{u}_s \gamma^\mu T^a u_t)$
Q_{HWB}	$H^\dagger \sigma^4 H W_{\mu\nu}^1 B^{\mu\nu}$	Q_{Hd}	$(H^\dagger i \overleftrightarrow{D}_\mu H) (\bar{d}_p \gamma^\mu d_r)$	$Q_{qd}^{(1)}$	$(\bar{q}_p \gamma_\mu q_r) (\bar{d}_s \gamma^\mu d_t)$
$Q_{H\bar{W}B}$	$H^\dagger \sigma^4 H \bar{W}_{\mu\nu}^1 B^{\mu\nu}$	$Q_{Hud} + \text{h.c.}$	$i(\bar{H}^\dagger D_\mu H) (\bar{u}_p \gamma^\mu d_r)$	$Q_{qd}^{(8)}$	$(\bar{q}_p \gamma_\mu T^a q_r) (\bar{d}_s \gamma^\mu T^a d_t)$
$\mathcal{L}_6^{(5)} - \psi^2 H^3$		$\mathcal{L}_6^{(8a)} - (\bar{L}L)(\bar{L}L)$		$\mathcal{L}_6^{(8d)} - (\bar{L}R)(\bar{R}L), (\bar{L}R)(\bar{L}R)$	
Q_{eH}	$(H^\dagger H) (\bar{l}_p e_r H)$	Q_{ll}	$(\bar{l}_p \gamma_\mu l_r) (\bar{l}_s \gamma^\mu l_t)$	Q_{leaq}	$(\bar{l}_j^k e_r) (\bar{d}_s q_{jt})$
Q_{uH}	$(H^\dagger H) (\bar{q}_p u_r \bar{H})$	$Q_{qq}^{(1)}$	$(\bar{q}_p \gamma_\mu q_r) (\bar{q}_s \gamma^\mu q_t)$	$Q_{quqd}^{(1)}$	$(\bar{q}_j^k u_r) \varepsilon_{jk} (\bar{q}_s^k d_t)$
Q_{dH}	$(H^\dagger H) (\bar{q}_p d_r H)$	$Q_{qq}^{(3)}$	$(\bar{q}_p \gamma_\mu \sigma^i q_r) (\bar{q}_s \gamma^\mu \sigma^i q_t)$	$Q_{quqd}^{(8)}$	$(\bar{q}_j^k T^a u_r) \varepsilon_{jk} (\bar{q}_s^k T^a d_t)$
		$Q_{lq}^{(1)}$	$(\bar{l}_p \gamma_\mu l_r) (\bar{q}_s \gamma^\mu q_t)$	$Q_{lequ}^{(1)}$	$(\bar{l}_j^k e_r) \varepsilon_{jk} (\bar{q}_s^k u_t)$
		$Q_{lq}^{(3)}$	$(\bar{l}_p \gamma_\mu \sigma^i l_r) (\bar{q}_s \gamma^\mu \sigma^i q_t)$	$Q_{lequ}^{(3)}$	$(\bar{l}_j^k \sigma_{\mu\nu} e_r) \varepsilon_{jk} (\bar{q}_s^k \sigma^{\mu\nu} u_t)$

- Use Warsaw basis
- Gauge boson self-interactions highlighted

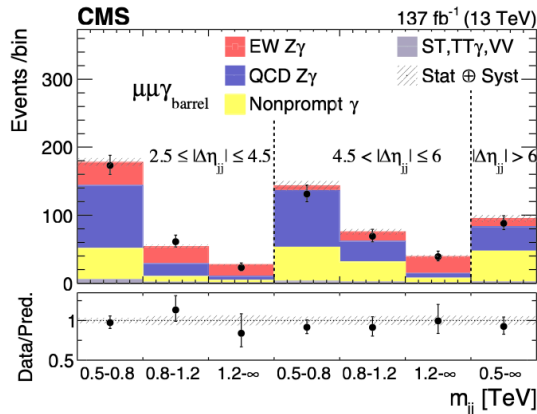
Full slew of Effective Field Theory operators at dimension-6

$\mathcal{L}_6^{(1)} - X^3$		$\mathcal{L}_6^{(6)} - \psi^2 XH$	$\mathcal{L}_6^{(8b)} - (\bar{R}R)(\bar{R}R)$		
Q_G	$f^{abc} G_{\mu\nu}^a G_{\nu\rho}^b G_{\rho\mu}^c$	Q_{eW}	$(\bar{l}_p \sigma^{\mu\nu} e_r) \sigma^i H W_{\mu\nu}^i$	Q_{ee}	$(\bar{e}_p \gamma_\mu e_r) (\bar{e}_s \gamma^\mu e_t)$
$Q_{\bar{G}}$	$f^{abc} \bar{G}_{\mu\nu}^a G_{\nu\rho}^b G_{\rho\mu}^c$	Q_{eB}	$(\bar{l}_p \sigma^{\mu\nu} e_r) H B_{\mu\nu}$	Q_{uu}	$(\bar{u}_p \gamma_\mu u_r) (\bar{u}_s \gamma^\mu u_t)$
Q_W	$\varepsilon^{ijk} W_{\mu\nu}^i W_{\nu\rho}^j W_{\rho\mu}^k$	Q_{uG}	$(\bar{q}_p \sigma^{\mu\nu} T^a u_r) \bar{H} G_{\mu\nu}^a$	Q_{dd}	$(\bar{d}_p \gamma_\mu d_r) (\bar{d}_s \gamma^\mu d_t)$
$Q_{\bar{W}}$	$\varepsilon^{ijk} \bar{W}_{\mu\nu}^i W_{\nu\rho}^j W_{\rho\mu}^k$	Q_{uW}	$(\bar{q}_p \sigma^{\mu\nu} u_r) \sigma^i \bar{H} W_{\mu\nu}^i$	Q_{eu}	$(\bar{e}_p \gamma_\mu e_r) (\bar{u}_s \gamma^\mu u_t)$
$\mathcal{L}_6^{(2)} - H^6$		Q_{uB}	$(\bar{q}_p \sigma^{\mu\nu} u_r) \bar{H} B_{\mu\nu}$	Q_{ed}	$(\bar{e}_p \gamma_\mu e_r) (\bar{d}_s \gamma^\mu d_t)$
Q_H	$(H^\dagger H)^3$	Q_{dG}	$(\bar{q}_p \sigma^{\mu\nu} T^a d_r) H G_{\mu\nu}^a$	$Q_{ud}^{(1)}$	$(\bar{u}_p \gamma_\mu u_r) (\bar{d}_s \gamma^\mu d_t)$
$\mathcal{L}_6^{(3)} - H^4 D^2$		Q_{dW}	$(\bar{q}_p \sigma^{\mu\nu} d_r) \sigma^i H W_{\mu\nu}^i$	$Q_{ud}^{(8)}$	$(\bar{u}_p \gamma_\mu T^a u_r) (\bar{d}_s \gamma^\mu T^a d_t)$
$Q_{H\Box}$	$(H^\dagger H) \Box (H^\dagger H)$	Q_{dB}	$(\bar{q}_p \sigma^{\mu\nu} d_r) H B_{\mu\nu}$		
Q_{HD}	$(D^\mu H^\dagger H) (H^\dagger D_\mu H)$				
$\mathcal{L}_6^{(4)} - X^2 H^2$		$\mathcal{L}_6^{(7)} - \psi^2 H^2 D$	$\mathcal{L}_6^{(8c)} - (\bar{L}L)(\bar{R}R)$		
Q_{HG}	$H^\dagger H G_{\mu\nu}^a G^{a\mu\nu}$	$Q_{HI}^{(1)}$	$(H^\dagger i \overleftrightarrow{D}_\mu H) (\bar{l}_p \gamma^\mu l_r)$	Q_{le}	$(\bar{l}_p \gamma_\mu l_r) (\bar{e}_s \gamma^\mu e_t)$
$Q_{H\bar{G}}$	$H^\dagger H \bar{G}_{\mu\nu}^a G^{a\mu\nu}$	$Q_{HI}^{(3)}$	$(H^\dagger i \overleftrightarrow{D}_\mu^\dagger H) (\bar{l}_p \sigma^i \gamma^\mu l_r)$	Q_{lu}	$(\bar{l}_p \gamma_\mu l_r) (\bar{u}_s \gamma^\mu u_t)$
Q_{HW}	$H^\dagger H W_{\mu\nu}^i W^{i\mu\nu}$	Q_{He}	$(H^\dagger i \overleftrightarrow{D}_\mu H) (\bar{e}_p \gamma^\mu e_r)$	Q_{ld}	$(\bar{l}_p \gamma_\mu l_r) (\bar{d}_s \gamma^\mu d_t)$
$Q_{H\bar{W}}$	$H^\dagger H \bar{W}_{\mu\nu}^i W^{i\mu\nu}$	$Q_{Hq}^{(1)}$	$(H^\dagger i \overleftrightarrow{D}_\mu H) (\bar{q}_p \gamma^\mu q_r)$	Q_{qe}	$(\bar{q}_p \gamma_\mu q_r) (\bar{e}_s \gamma^\mu e_t)$
Q_{HB}	$H^\dagger H B_{\mu\nu} B^{\mu\nu}$	$Q_{Hq}^{(3)}$	$(H^\dagger i \overleftrightarrow{D}_\mu^\dagger H) (\bar{q}_p \sigma^i \gamma^\mu q_r)$	$Q_{qu}^{(1)}$	$(\bar{q}_p \gamma_\mu q_r) (\bar{u}_s \gamma^\mu u_t)$
$Q_{H\bar{B}}$	$H^\dagger H \bar{B}_{\mu\nu} B^{\mu\nu}$	Q_{Hu}	$(H^\dagger i \overleftrightarrow{D}_\mu H) (\bar{u}_p \gamma^\mu u_r)$	$Q_{qu}^{(8)}$	$(\bar{q}_p \gamma_\mu T^a q_r) (\bar{u}_s \gamma^\mu T^a u_t)$
Q_{HWB}	$H^\dagger \sigma^i H W_{\mu\nu}^i B^{\mu\nu}$	Q_{Hd}	$(H^\dagger i \overleftrightarrow{D}_\mu H) (\bar{d}_p \gamma^\mu d_r)$	$Q_{qd}^{(1)}$	$(\bar{q}_p \gamma_\mu q_r) (\bar{d}_s \gamma^\mu d_t)$
$Q_{H\bar{W}B}$	$H^\dagger \sigma^i H \bar{W}_{\mu\nu}^i B^{\mu\nu}$	$Q_{Hud} + \text{h.c.}$	$i(\bar{H}^\dagger D_\mu H) (\bar{u}_p \gamma^\mu d_r)$	$Q_{qd}^{(8)}$	$(\bar{q}_p \gamma_\mu T^a q_r) (\bar{d}_s \gamma^\mu T^a d_t)$
$\mathcal{L}_6^{(5)} - \psi^2 H^3$		$\mathcal{L}_6^{(8a)} - (\bar{L}L)(\bar{L}L)$	$\mathcal{L}_6^{(8d)} - (\bar{L}R)(\bar{R}L), (\bar{L}R)(\bar{L}R)$		
Q_{eH}	$(H^\dagger H) (\bar{l}_p e_r H)$	Q_{ll}	$(\bar{l}_p \gamma_\mu l_r) (\bar{l}_s \gamma^\mu l_t)$	$Q_{le dq}$	$(\bar{l}_p e_r) (\bar{d}_s q_{tj})$
Q_{uH}	$(H^\dagger H) (\bar{q}_p u_r \bar{H})$	$Q_{qq}^{(1)}$	$(\bar{q}_p \gamma_\mu q_r) (\bar{q}_s \gamma^\mu q_t)$	$Q_{quqd}^{(1)}$	$(\bar{q}_p^j u_r) \varepsilon_{jk} (\bar{q}_s^k d_t)$
Q_{dH}	$(H^\dagger H) (\bar{q}_p d_r H)$	$Q_{qq}^{(3)}$	$(\bar{q}_p \gamma_\mu \sigma^i q_r) (\bar{q}_s \gamma^\mu \sigma^i q_t)$	$Q_{quqd}^{(8)}$	$(\bar{q}_p^j T^a u_r) \varepsilon_{jk} (\bar{q}_s^k T^a d_t)$
		$Q_{lq}^{(1)}$	$(\bar{l}_p \gamma_\mu l_r) (\bar{q}_s \gamma^\mu q_t)$	$Q_{lequ}^{(1)}$	$(\bar{l}_p e_r) \varepsilon_{jk} (\bar{q}_s^k u_t)$
		$Q_{lq}^{(3)}$	$(\bar{l}_p \gamma_\mu \sigma^i l_r) (\bar{q}_s \gamma^\mu \sigma^i q_t)$	$Q_{lequ}^{(3)}$	$(\bar{l}_p \sigma_{\mu\nu} e_r) \varepsilon_{jk} (\bar{q}_s^k \sigma^{\mu\nu} u_t)$

- Use Warsaw basis
- Gauge boson self-interactions highlighted

VBS Z γ

- $\ell+\ell-\gamma jj$ final states ($\ell = e$ or μ)
- Main background QCD-induced Z γjj , from simulation, constrained in data
- Z+jets with selected photon is not prompt, data-driven
- Cross section in the fiducial volume
 - EW Z γjj : $5.21 \pm 0.52(\text{stat}) \pm 0.56(\text{syst})$ fb
 - EW and QCD-induced Z γjj : $14.7 \pm 0.80(\text{stat}) \pm 1.26(\text{syst})$ fb



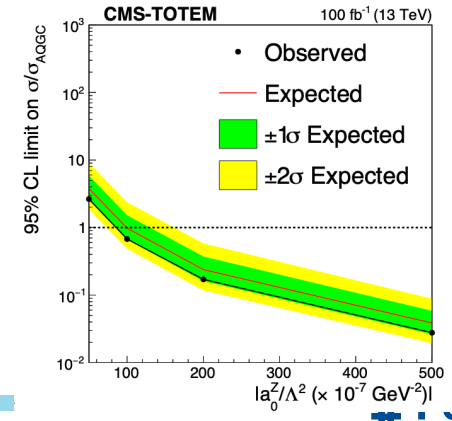
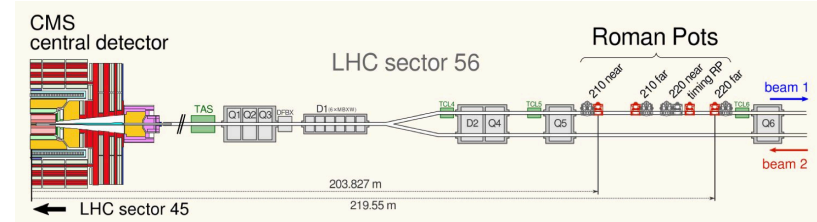
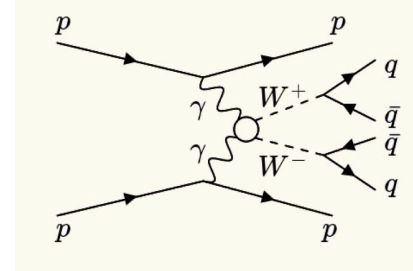
Common selection	$p_T^{\ell^1, \ell^2} > 25 \text{ GeV}$, $ \eta^{\ell^1, \ell^2} < 2.5$ for electron channel $p_T^{\ell^1, \ell^2} > 20 \text{ GeV}$, $ \eta^{\ell^1, \ell^2} < 2.4$ for muon channel $p_T^\gamma > 20 \text{ GeV}$, $ \eta^\gamma < 1.442$ or $1.566 < \eta^\gamma < 2.500$ $p_T^{j1, j2} > 30 \text{ GeV}$, $ \eta^{j1, j2} < 4.7$ $70 < m_{\ell\ell} < 110 \text{ GeV}$, $m_{Z\gamma} > 100 \text{ GeV}$ $\Delta R_{jj}, \Delta R_{j\gamma}, \Delta R_{j\ell} > 0.5$, $\Delta R_{\ell\gamma} > 0.7$
Fiducial volume	Common selection, $m_{jj} > 500 \text{ GeV}$, $ \Delta\eta_{jj} > 2.5$
Control region	Common selection, $150 < m_{jj} < 500 \text{ GeV}$
EW signal region	Common selection, $m_{jj} > 500 \text{ GeV}$, $ \Delta\eta_{jj} > 2.5$, $\eta^* < 2.4$, $\Delta\phi_{Z\gamma, jj} > 1.9$
aQGC search region	Common selection, $m_{jj} > 500 \text{ GeV}$, $ \Delta\eta_{jj} > 2.5$, $p_T^\gamma > 120 \text{ GeV}$

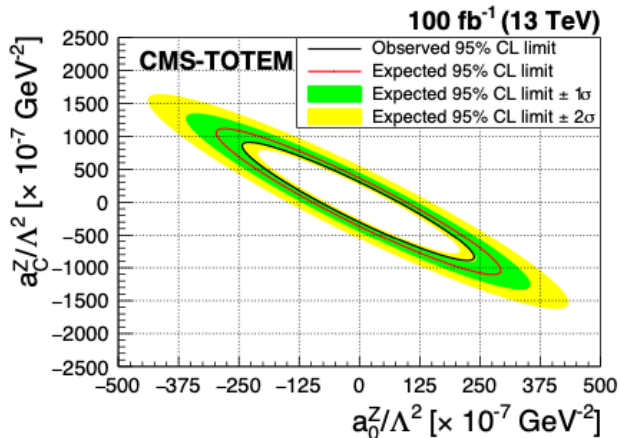
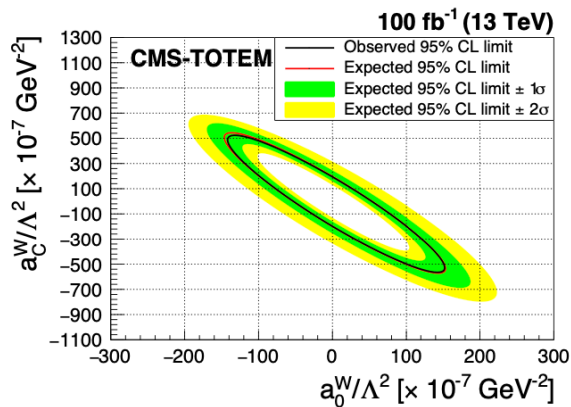
Coupling	Exp. lower	Exp. upper	Obs. lower	Obs. upper	Unitarity bound
F_{M0}/Λ^4	-12.5	12.8	-15.8	16.0	1.3
F_{M1}/Λ^4	-28.1	27.0	-35.0	34.7	1.5
F_{M2}/Λ^4	-5.21	5.12	-6.55	6.49	1.5
F_{M3}/Λ^4	-10.2	10.3	-13.0	13.0	1.8
F_{M4}/Λ^4	-10.2	10.2	-13.0	12.7	1.7
F_{M5}/Λ^4	-17.6	16.8	-22.2	21.3	1.7
F_{M7}/Λ^4	-44.7	45.0	-56.6	55.9	1.6
F_{T0}/Λ^4	-0.52	0.44	-0.64	0.57	1.9
F_{T1}/Λ^4	-0.65	0.63	-0.81	0.90	2.0
F_{T2}/Λ^4	-1.36	1.21	-1.68	1.54	1.9
F_{T5}/Λ^4	-0.45	0.52	-0.58	0.64	2.2
F_{T6}/Λ^4	-1.02	1.07	-1.30	1.33	2.0
F_{T7}/Λ^4	-1.67	1.97	-2.15	2.43	2.2
F_{T8}/Λ^4	-0.36	0.36	-0.47	0.47	1.8
F_{T9}/Λ^4	-0.72	0.72	-0.91	0.91	1.9



- ξ : fractional momentum loss of forward proton > 0.05
- Standard VV selection and $m_{j1} + m_{j2}$ to distinguish WW from ZZ
- Proton-jet matching requirements
- Data-driven bkg estimation in 3 SBs
 - 2 jets (QCD, V+jets, ttbar)
 - Protons from pileup/diffractive collisions or fake proton tracks from showers/beam bckg
- Main uncertainties: jet energy scale, proton ξ measurement, proton reconstruction efficiency, and integrated luminosity
- ML fit in 12 bins: 3 years, WW vs ZZ SR and 2 or 1 signal protons

Precision Proton Spectrometer (PPS)





Coupling	Observed (expected) 95% CL upper limit No clipping	Observed (expected) 95% CL upper limit Clipping at 1.4 TeV
$ a_0^W / \Lambda^2 $	4.3 (3.9) $\times 10^{-6}$ GeV ⁻²	5.2 (5.1) $\times 10^{-6}$ GeV ⁻²
$ a_C^W / \Lambda^2 $	1.6 (1.4) $\times 10^{-5}$ GeV ⁻²	2.0 (2.0) $\times 10^{-5}$ GeV ⁻²
$ a_0^Z / \Lambda^2 $	0.9 (1.0) $\times 10^{-5}$ GeV ⁻²	—
$ a_C^Z / \Lambda^2 $	4.0 (4.5) $\times 10^{-5}$ GeV ⁻²	—

Dim-6

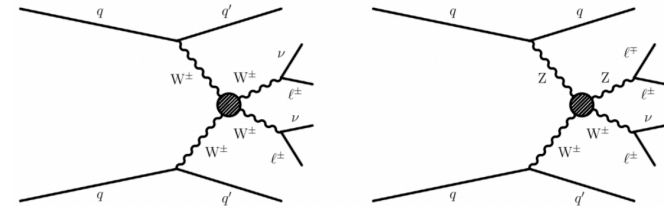
$$a_0^W = -\frac{m_W}{\pi\alpha_{em}} \left[s_w^2 \frac{f_{M,0}}{\Lambda^2} + 2c_w^2 \frac{f_{M,2}}{\Lambda^2} + s_w c_w \frac{f_{M,4}}{\Lambda^2} \right]$$

Translated

Dim-8

Coupling	Observed (expected) 95% CL upper limit No clipping	Observed (expected) 95% CL upper limit Clipping at 1.4 TeV
$ f_{M,0} / \Lambda^4 $	66.0 (60.0) TeV ⁻⁴	79.8 (78.2) TeV ⁻⁴
$ f_{M,1} / \Lambda^4 $	245.5 (214.8) TeV ⁻⁴	306.8 (306.8) TeV ⁻⁴
$ f_{M,2} / \Lambda^4 $	9.8 (9.0) TeV ⁻⁴	11.9 (11.8) TeV ⁻⁴
$ f_{M,3} / \Lambda^4 $	73.0 (64.6) TeV ⁻⁴	91.3 (92.3) TeV ⁻⁴
$ f_{M,4} / \Lambda^4 $	36.0 (32.9) TeV ⁻⁴	43.5 (42.9) TeV ⁻⁴
$ f_{M,5} / \Lambda^4 $	67.0 (58.9) TeV ⁻⁴	83.7 (84.1) TeV ⁻⁴
$ f_{M,7} / \Lambda^4 $	490.9 (429.6) TeV ⁻⁴	613.7 (613.7) TeV ⁻⁴

$$z_\ell^* = \left| \eta^\ell - \frac{\eta^{j1} + \eta^{j2}}{2} \right| / |\Delta\eta_{jj}|$$



- Background estimation with CR in data & simulation
- Simultaneous fit of WZ and $W_\pm W_\pm$ SR
- data-to-simulation efficiency correction for charge-misidentified electron

Variable	$W^\pm W^\pm$	WZ
Leptons	2 leptons, $p_T > 25/20$ GeV	3 leptons, $p_T > 25/10/20$ GeV
p_T^j	> 50 GeV	> 50 GeV
$ m_{\ell\ell} - m_Z $	> 15 GeV (ee)	< 15 GeV
$m_{\ell\ell}$	> 20 GeV	—
$m_{\ell\ell\ell}$	—	> 100 GeV
p_T^{miss}	> 30 GeV	> 30 GeV
b quark veto	Required	Required
$\max(z_\ell^*)$	< 0.75	< 1.0
m_{jj}	> 500 GeV	> 500 GeV
$ \Delta\eta_{jj} $	> 2.5	> 2.5

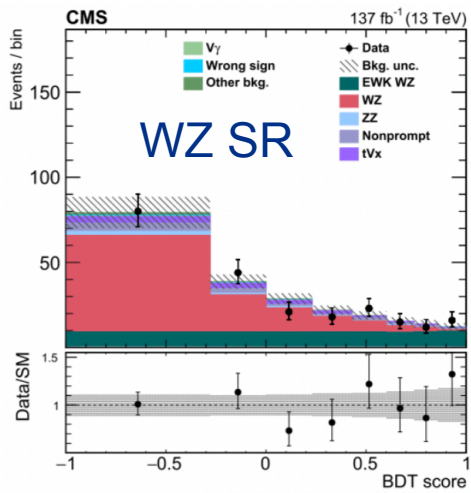
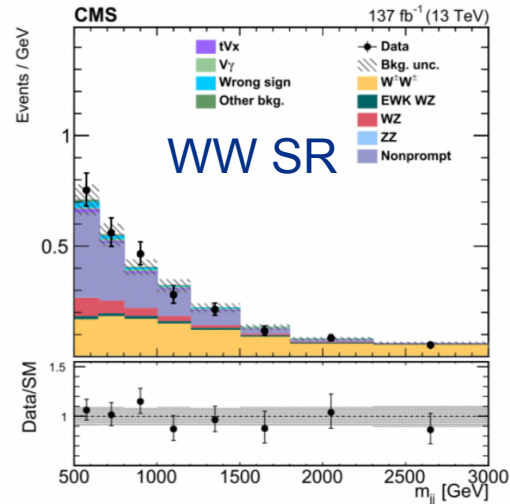
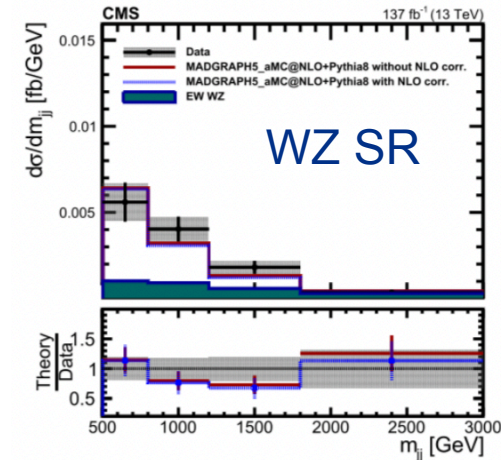
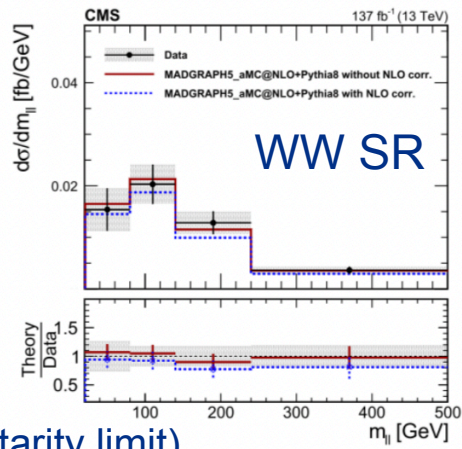


Table 3

List and description of all the input variables used in the BDT analysis for the WZ SR.

Variable	Definition
m_{jj}	Mass of the leading and trailing jets system
$ \Delta\eta_{jj} $	Absolute difference in rapidity of the leading and trailing jets
$\Delta\phi_{jj}$	Absolute difference in azimuthal angles of the leading and trailing jets
p_T^{j1}	p_T of the leading jet
p_T^{j2}	p_T of the trailing jet
η^{j1}	Pseudorapidity of the leading jet
$ \eta^W - \eta^Z $	Absolute difference between the rapidities of the Z boson and the charged lepton from the decay of the W boson
$z_{\ell_i}^*$ ($i = 1 - 3$)	Zeppenfeld variable of the three selected leptons
$z_{3\ell}^*$	Zeppenfeld variable of the vector sum of the three leptons
$\Delta R_{j1,Z}$	ΔR between the leading jet and the Z boson
$ \vec{p}_T^{\text{tot}} / \sum_i p_T^i$	Transverse component of the vector sum of the bosons and tagging jets momenta, normalized to their scalar p_T sum

- EW WZ obs. (exp.) significance 6.8 (5.3)
- EW $W_{\pm}W_{\pm}$ signal \gg 5 standard deviations



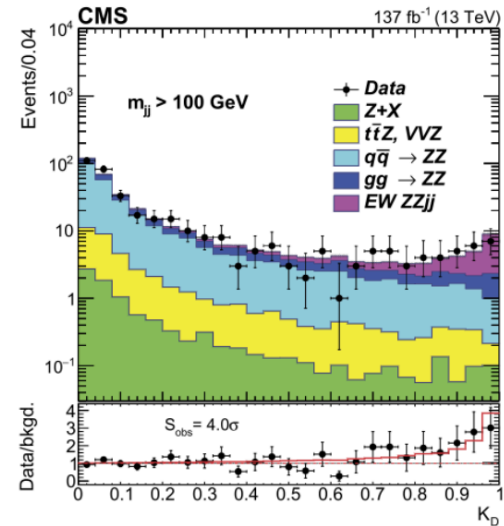
Dim-8 limits (cutting the EFT expansion at the unitarity limit)

	Observed ($W^{\pm}W^{\pm}$) (TeV^{-4})	Expected ($W^{\pm}W^{\pm}$) (TeV^{-4})	Observed (WZ) (TeV^{-4})	Expected (WZ) (TeV^{-4})	Observed (TeV^{-4})	Expected (TeV^{-4})
f_{T0}/Λ^4	[-1.5, 2.3]	[-2.1, 2.7]	[-1.6, 1.9]	[-2.0, 2.2]	[-1.1, 1.6]	[-1.6, 2.0]
f_{T1}/Λ^4	[-0.81, 1.2]	[-0.98, 1.4]	[-1.3, 1.5]	[-1.6, 1.8]	[-0.69, 0.97]	[-0.94, 1.3]
f_{T2}/Λ^4	[-2.1, 4.4]	[-2.7, 5.3]	[-2.7, 3.4]	[-4.4, 5.5]	[-1.6, 3.1]	[-2.3, 3.8]
f_{M0}/Λ^4	[-13, 16]	[-19, 18]	[-16, 16]	[-19, 19]	[-11, 12]	[-15, 15]
f_{M1}/Λ^4	[-20, 19]	[-22, 25]	[-19, 20]	[-23, 24]	[-15, 14]	[-18, 20]
f_{M6}/Λ^4	[-27, 32]	[-37, 37]	[-34, 33]	[-39, 39]	[-22, 25]	[-31, 30]
f_{M7}/Λ^4	[-22, 24]	[-27, 25]	[-22, 22]	[-28, 28]	[-16, 18]	[-22, 21]
f_{S0}/Λ^4	[-35, 36]	[-31, 31]	[-83, 85]	[-88, 91]	[-34, 35]	[-31, 31]
f_{S1}/Λ^4	[-100, 120]	[-100, 110]	[-110, 110]	[-120, 130]	[-86, 99]	[-91, 97]

VBS ZZ

Fully leptonic

- Main bckg: production of 2Z bosons + QCD-induced jets, estimated from simulation but further constrained in data
- Other irreducible bckgs: processes with high-pT isolated leptons $t\bar{t}Z$ +jets and VVZ +jets, from simulation
- Reducible bckgs: heavy-flavor jets produce secondary leptons or jets misidentified as leptons as Z +jets, $t\bar{t}$ +jets and WZ +jets
- Main unc: QCD renormalization and factorization scales (signal) and jet energy scale $\sim 10\%$
- signal strength for the EW production,
- $\mu = \sigma / \sigma_{\text{SM}}$, extracted with matrix element discriminant (KD)



Coupling	Exp. lower	Exp. upper	Obs. lower	Obs. upper	Unitarity bound
f_{T0}/Λ^4	-0.37	0.35	-0.24 (-0.26)	0.22 (0.24)	2.4
f_{T1}/Λ^4	-0.49	0.49	-0.31 (-0.34)	0.31 (0.34)	2.6
f_{T2}/Λ^4	-0.98	0.95	-0.63 (-0.69)	0.59 (0.65)	2.5
f_{T8}/Λ^4	-0.68	0.68	-0.43 (-0.47)	0.43 (0.48)	1.8
f_{T9}/Λ^4	-1.5	1.5	-0.92 (-1.02)	0.92 (1.02)	1.8

Best

- Electron charge misidentification in simulation is corrected to reproduce the rate measured in data, using $Z \rightarrow ee$ events: mis. rate is about 0.01% (0.3%) in the barrel (endcap) region. Contri [50]. Contribution in OS dilepton final states from $t\bar{t}$, tW , $W+W-$, and Drell–Yan
- CRs to estimate the normalization of the main backgrounds from data: WZ , nonprompt lepton, tZq , and ZZ
- 2 fits are performed for the cross-sections on 2D variable (inclusive + signal BDTs)
 - $WL_{\pm} WL_{\pm}$ and $WX_{\pm} WT_{\pm}$
 - $WL_{\pm} WX_{\pm}$ and $WT_{\pm} WT_{\pm}$

Process	σB (fb)	Theoretical prediction (fb)
$W_L^{\pm} W_L^{\pm}$	$0.32^{+0.42}_{-0.40}$	0.44 ± 0.05
$W_X^{\pm} W_T^{\pm}$	$3.06^{+0.51}_{-0.48}$	3.13 ± 0.35
$W_L^{\pm} W_X^{\pm}$	$1.20^{+0.56}_{-0.53}$	1.63 ± 0.18
$W_T^{\pm} W_T^{\pm}$	$2.11^{+0.49}_{-0.47}$	1.94 ± 0.21
$W_L^{\pm} W_L^{\pm}$	$0.24^{+0.44}_{-0.37}$	0.28 ± 0.03
$W_X^{\pm} W_T^{\pm}$	$3.25^{+0.50}_{-0.48}$	3.32 ± 0.37
$W_L^{\pm} W_X^{\pm}$	$1.40^{+0.60}_{-0.57}$	1.71 ± 0.19
$W_T^{\pm} W_T^{\pm}$	$2.03^{+0.51}_{-0.50}$	1.89 ± 0.21

WW RF

obs. (exp.) significance
 $WL_{\pm} WX_{\pm} 2.3 (3.1)$

Partons
 RF

obs. (exp.) significance
 $WL_{\pm} WX_{\pm} 2.6 (2.9)$

Variables	Definitions
$\Delta\phi_{jj}$	Difference in azimuthal angle between the leading and subleading jets
p_T^{j1}	p_T of the leading jet
p_T^{j2}	p_T of the subleading jet
$p_T^{\ell_1}$	Leading lepton p_T
$p_T^{\ell_2}$	Subleading lepton p_T
$\Delta\phi_{\ell\ell}$	Difference in azimuthal angle between the two leptons
$m_{\ell\ell}$	Dilepton mass
$p_T^{\ell\ell}$	Dilepton p_T
m_T^{WW}	Transverse WW diboson mass
$Z_{\ell_1}^*$	Zeppenfeld variable of the leading lepton
$Z_{\ell_2}^*$	Zeppenfeld variable of the subleading lepton
$\Delta R_{j1,\ell\ell}$	ΔR between the leading jet and the dilepton system
$\Delta R_{j2,\ell\ell}$	ΔR between the subleading jet and the dilepton system
$(p_T^{\ell_1} p_T^{\ell_2}) / (p_T^{j1} p_T^{j2})$	Ratio of p_T products between leptons and jets
p_T^{miss}	Missing transverse momentum

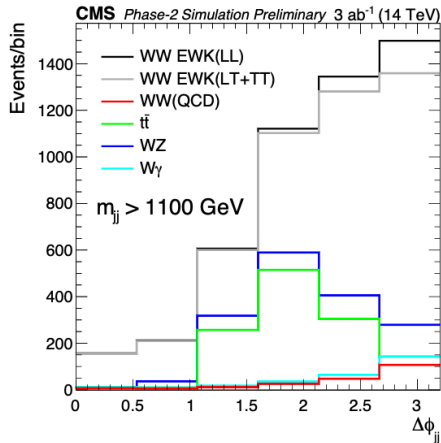
Source of uncertainty	$W_L^{\pm} W_L^{\pm}$ (%)	$W_X^{\pm} W_T^{\pm}$ (%)	$W_L^{\pm} W_X^{\pm}$ (%)	$W_T^{\pm} W_T^{\pm}$ (%)
Integrated luminosity	3.2	1.8	1.9	1.8
Lepton measurement	3.6	1.9	2.5	1.8
Jet energy scale and resolution	11	2.9	2.5	1.1
Pileup	0.9	0.1	1.0	0.3
b tagging	1.1	1.2	1.4	1.1
Nonprompt lepton rate	17	2.7	9.3	1.6
Trigger	1.9	1.1	1.6	0.9
Limited sample size	38	3.9	14	5.7
Theory	6.8	2.3	4.0	2.3
Total systematic uncertainty	44	6.6	18	7.0
Statistical uncertainty	123	15	42	22
Total uncertainty	130	16	46	23

Polarization

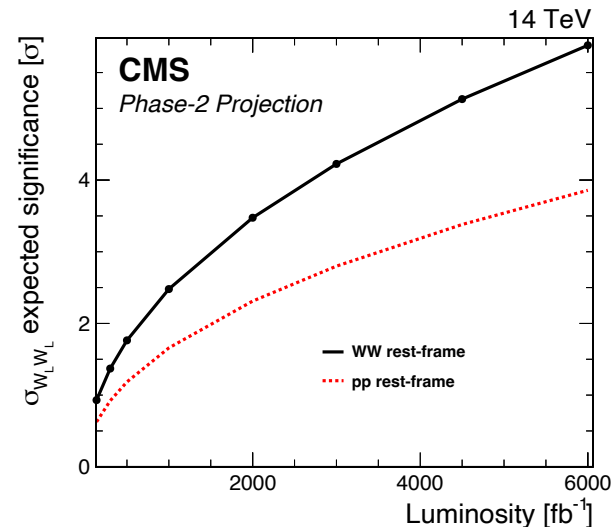
Fully leptonic

[CMS-PAS-FTR-21-001]

Simultaneous fit of $D\phi_{jj}$ variable in two m_{jj} regions

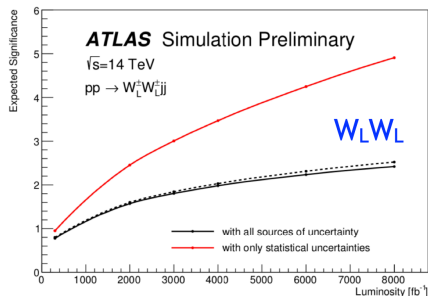
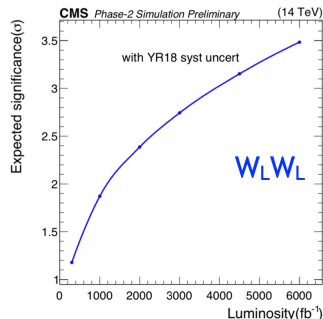


From 3 to 4 sigma at 3000/fb!



[CERN-LPCC-2018-03]

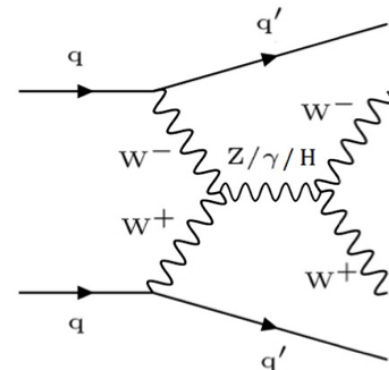
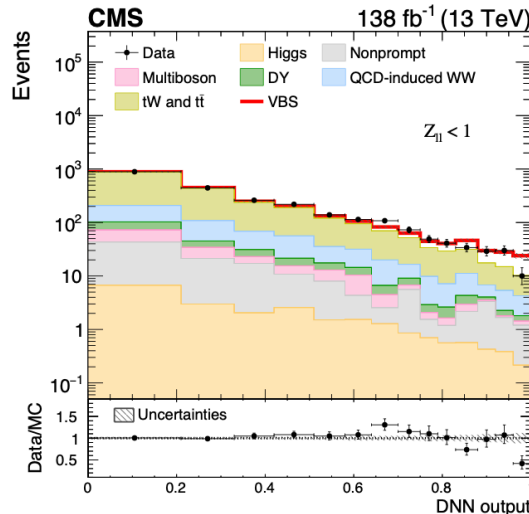
$Z_L Z_L$	significance	
	w/ syst. uncert.	w/o syst. uncert.
HL-LHC	1.4σ	1.4σ
HE-LHC	5.2σ	5.7σ



VBS osWW Fully leptonic

- VBS SR in 3 channels ee , $\mu\mu$, $e\mu$
- DY & $t\bar{t}$ CR
- Dedicated DNN for the $e\mu$ channel
- Signal strength from fit in SR+CR

[arXiv:2205.05711]



Inclusive cross section
 $99 \pm 20 \text{ fb}$ ($89 \pm 5 \text{ fb}$ theory)

Fiducial cross section
 $10.2 \pm 2.0 \text{ fb}$ ($9.1 \pm 0.6 \text{ fb}$ theory)

Objects	Requirements
	$e\mu, ee, \mu\mu$ (not from τ decay), opposite charge
	$p_T^{\text{dressed } \ell} = p_T^\ell + \sum_i p_T^{j_i}$ if $\Delta R(\ell, \gamma_i) < 0.1$
Leptons	$p_T^{\ell_1} > 25 \text{ GeV}, p_T^{\ell_2} > 13 \text{ GeV}, p_T^{\ell_3} < 10 \text{ GeV}$ $ \eta < 2.5$ $p_T^{\ell\ell} > 30 \text{ GeV}, m_{\ell\ell} > 50 \text{ GeV}$
	$p_T^j > 30 \text{ GeV}$ $\Delta R(j, \ell) > 0.4$
Jets	At least 2 jets, no b jets $ \eta < 4.7$ $m_{jj} > 300 \text{ GeV}, \Delta\eta_{jj} > 2.5$
	$p_T^{\text{miss}} > 20 \text{ GeV}$

$e\mu$ DNN

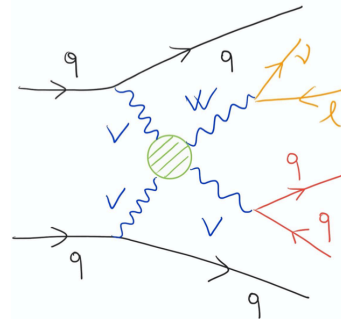
Variable	Description
m_{jj}	Invariant mass of the two tagging jets pair
$\Delta\eta_{jj}$	Pseudorapidity separation between the two tagging jets
p_T^1	p_T of the highest p_T jet
p_T^2	p_T of the second-highest p_T jet
$p_T^{\ell\ell}$	p_T of the lepton pair
$\Delta\phi_{\ell\ell}$	Azimuthal angle between the two leptons
Z_{ℓ_1}	Zeppenfeld variable of the highest p_T lepton
Z_{ℓ_2}	Zeppenfeld variable of the second-highest p_T lepton
$m_T^{\ell_1}$	Transverse mass of the $(p_T^{\ell_1}, p_T^{\text{miss}})$ system

Fiducial volume: Requirements at Gen level

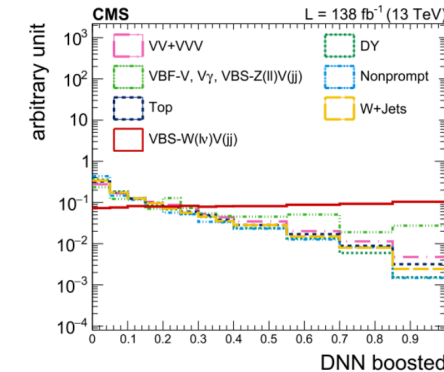
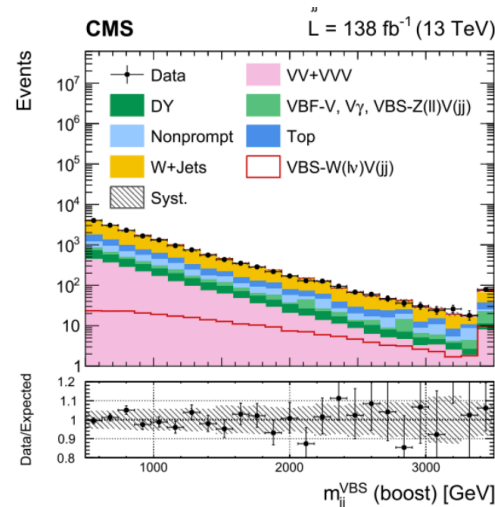
VBS WV (SM)

semi-leptonic

- Large BR but large irreducible backgrounds
- No public predictions beyond LO accuracy for semileptonic signatures
- Advances in signal modeling of parton-shower effects (Dipole recoil scheme used for the first time) [[arXiv:1710.00391](https://arxiv.org/abs/1710.00391)]
- Data-driven bkg estimation for Top and W+jets backgrounds:
 - Top: one free floating parameter per category in the ML fit
 - Wjets: several free floating parameters per category in the ML fit, to perfect the modeling of VBS-jets momenta.
- Main uncertainties: statistical, theoretical and b-tagging

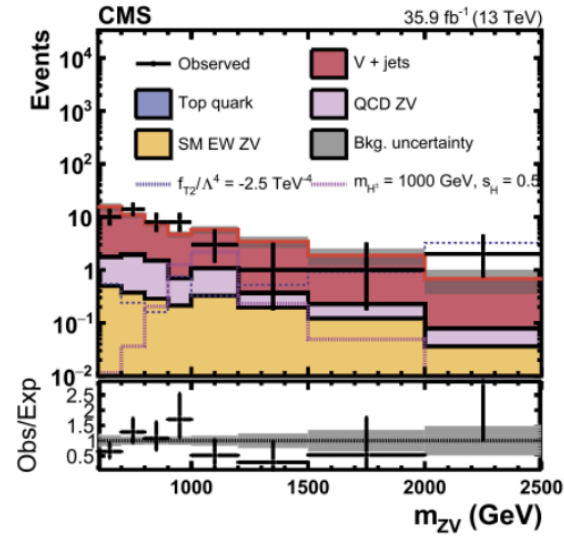


Boosted & resolved categories



Variable	Resolved	Boosted	SHAP ranking	
			Resolved	Boosted
Lepton pseudorapidity	✓	✓	13	12
Lepton transverse momentum	✓	✓	16	10
Zeppenfeld variable for the lepton	✓	✓	2	2
Number of jets with $p_T > 30 \text{ GeV}$	✓	✓	7	3
Leading VBS tag jet p_T	-	✓	-	11
Trailing VBS tag jet p_T	✓	✓	7	6
Pseudorapidity interval $\Delta\eta_{\text{VBS}}$ between tag jets	✓	✓	4	4
Quark/gluon discriminator of leading VBS tag jet	✓	✓	9	7
Azimuthal angle distance between VBS tag jets	✓	✓	10	-
Invariant mass of the VBS tag jets pair	✓	✓	1	1
p_T of the leading V_{had} jet	✓	-	14	-
p_T of the trailing V_{had} jet	✓	-	12	-
Pseudorapidity difference between V_{had} jets	✓	-	8	-
Quark/gluon discriminator of the leading V_{had} jet	✓	-	3	-
Quark/gluon discriminator of the trailing V_{had} jet	✓	-	5	-
p_T of the AK8 jet candidate	✓	✓	-	8
Invariant mass of V_{had}	✓	✓	11	5
Zeppenfeld variable for V_{had}	-	✓	-	9
Centrality	-	✓	15	13

- Includes also a search for charged Higgs bosons
- Main bckg V+jets from data is SB region
 - Fit of the mwv & mzv & obtain transfer factor
- Unitarity constraints not included
- First aQGC search in this channel



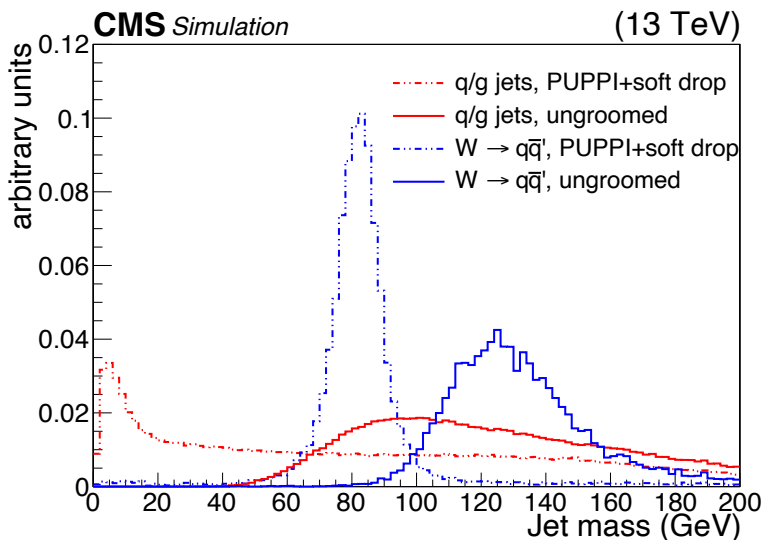
	Observed (WV) (TeV ⁻⁴)	Expected (WV) (TeV ⁻⁴)	Observed (ZV) (TeV ⁻⁴)	Expected (ZV) (TeV ⁻⁴)	Observed (TeV ⁻⁴)	Expected (TeV ⁻⁴)
f_{S0}/Λ^4	[-2.7, 2.7]	[-4.2, 4.2]	[-40, 40]	[-31, 31]	[-2.7, 2.7]	[-4.2, 4.2]
f_{S1}/Λ^4	[-3.3, 3.4]	[-5.2, 5.2]	[-32, 32]	[-24, 24]	[-3.4, 3.4]	[-5.2, 5.2]
f_{M0}/Λ^4	[-0.69, 0.69]	[-1.0, 1.0]	[-7.5, 7.5]	[-5.3, 5.3]	[-0.69, 0.70]	[-1.0, 1.0]
f_{M1}/Λ^4	[-2.0, 2.0]	[-3.0, 3.0]	[-22, 23]	[-16, 16]	[-2.0, 2.1]	[-3.0, 3.0]
f_{M6}/Λ^4	[-1.4, 1.4]	[-2.0, 2.0]	[-15, 15]	[-11, 11]	[-1.3, 1.3]	[-1.4, 1.4]
f_{M7}/Λ^4	[-3.4, 3.4]	[-5.1, 5.1]	[-35, 36]	[-25, 26]	[-3.4, 3.4]	[-5.1, 5.1]
f_{T0}/Λ^4	[-0.12, 0.11]	[-0.17, 0.16]	[-1.4, 1.4]	[-1.0, 1.0]	[-0.12, 0.11]	[-0.17, 0.16]
f_{T1}/Λ^4	[-0.12, 0.13]	[-0.18, 0.18]	[-1.5, 1.5]	[-1.0, 1.0]	[-0.12, 0.13]	[-0.18, 0.18]
f_{T2}/Λ^4	[-0.28, 0.28]	[-0.41, 0.41]	[-3.4, 3.4]	[-2.4, 2.4]	[-0.28, 0.28]	[-0.41, 0.41]

Softdrop

- Soft drop: reduce the jet contamination from initial state radiation, underlying event and pileup

Soft drop condition:
$$\frac{\min(p_{T1}, p_{T2})}{p_{T1} + p_{T2}} > z_{\text{cut}} \left(\frac{\Delta R_{12}}{R} \right)^\beta$$

1. Jet j clustered with CA
2. Decluster last step and obtain j_1 and j_2
3. Check if soft drop condition is satisfied



Yes

j is the final
SD jet

No

decluster jet with higher p_T ,
remove the other,
Repeat

[B2G-17-001]

Nsubjettiness

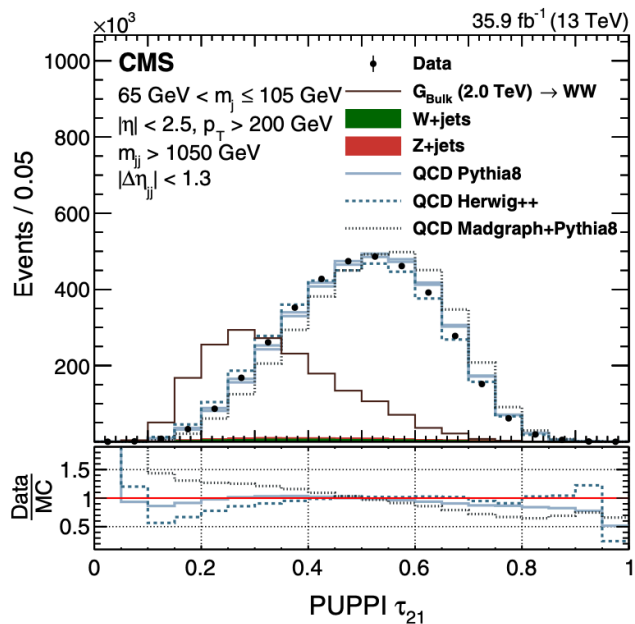
[arXiv:1011.2268]

- N-subjettiness τ_N tells how likely a jet has N subjets

$$\tau_N = \frac{1}{d_0} \sum_k p_{T,k} \min\{\Delta R_{1,k}, \Delta R_{2,k}, \dots, \Delta R_{N,k}\} \quad d_0 = \sum_k p_{T,k} R$$

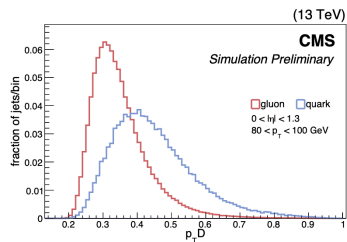
N = identified subjets
k = jet constituents

[B2G-17-001]

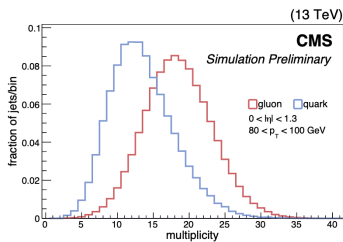


- $\tau_N \sim 0$: N subjets likely
- $\tau_N \gg 0$: more than N subjets likely

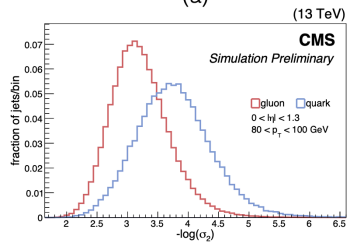
QG likelihood [CMS DP -2016/070]



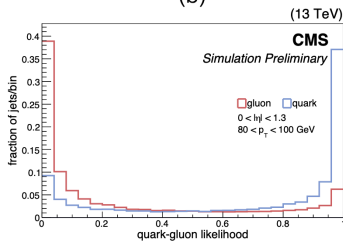
(a)



(b)



(c)



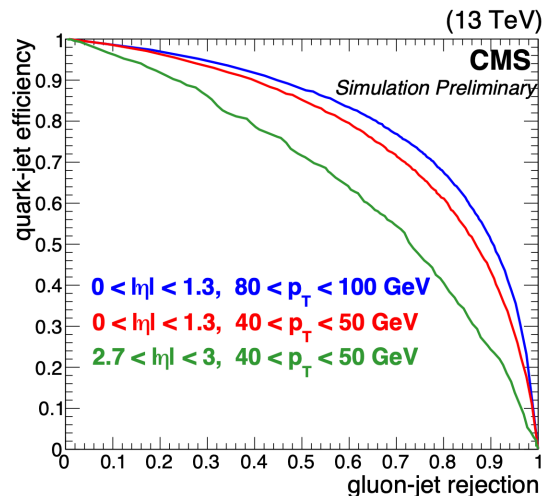
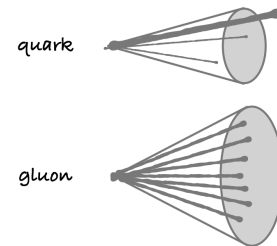
(d)

Quark-gluon discrimination variables from simulation: (a) $p_T D = \frac{\sqrt{\sum_i p_{T,i}^2}}{\sum_i p_{T,i}}$ (b) multiplicity (c) $-\log(\sigma_2)$, where σ_2 is the ellipse minor axis (d) the Quark-Gluon Likelihood.

3

Main differences are:

- the **particle multiplicity** is higher in gluon jets than in light-quark jets;
- the **fragmentation function** of gluon jets is considerably softer than that of a quark jet;
- gluon jets are less **collimated** than quark jets.

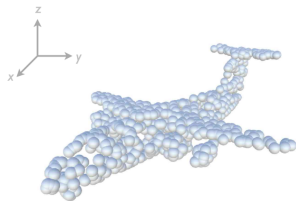


ParticleNet

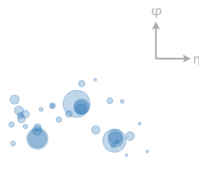
[[Phys. Rev. D 101 \(2020\) 056019](#)]

- Customized neural network architecture based on the particle cloud representation → jet as an unordered set of particles
 - Uses a permutation-invariant graph neural network architecture
- In CMS:
 - multi-class tagger for t/W/Z/H tagging
 - same inputs as DeepAK8 (PF candidates/secondary vertices)
 - significant performance improvement
 - Mass decorrelation obtained with training using a dedicated signal sample with flat mass spectrum: $m_X \in [15, 250]$ GeV

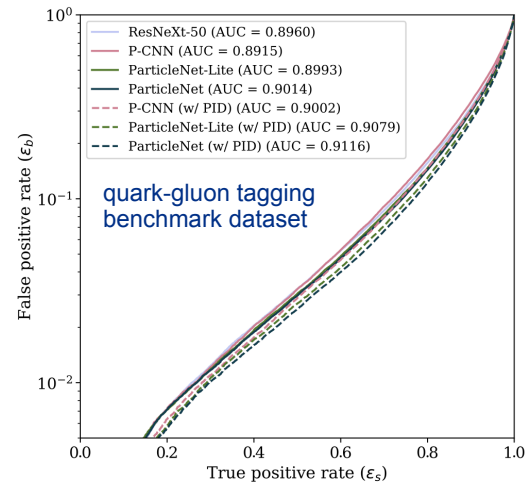
de Clouds - April 17, 2019 - Hulin Qu (UCSB)



- Point cloud
 - points are intrinsically *unordered*
 - primary information:
 - 3D coordinates in the xyz space

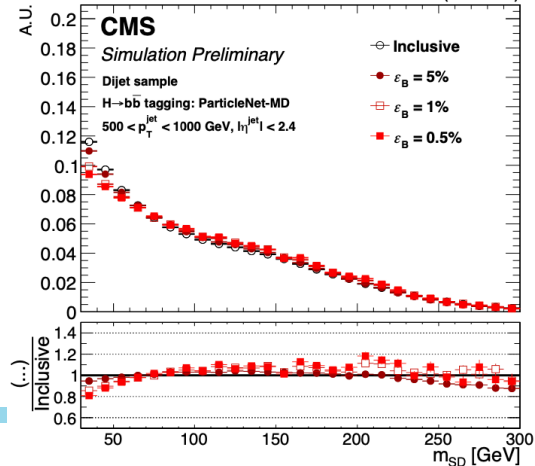


- Particle cloud
 - particles are intrinsically *unordered*
 - primary information:
 - 2D coordinates in the η - ϕ space
- Plus all other particle properties as momentum, charge, etc.

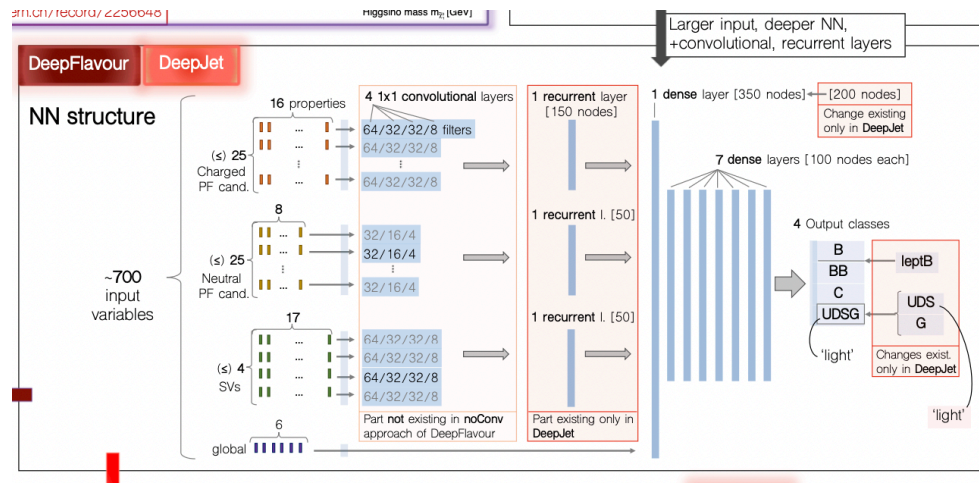
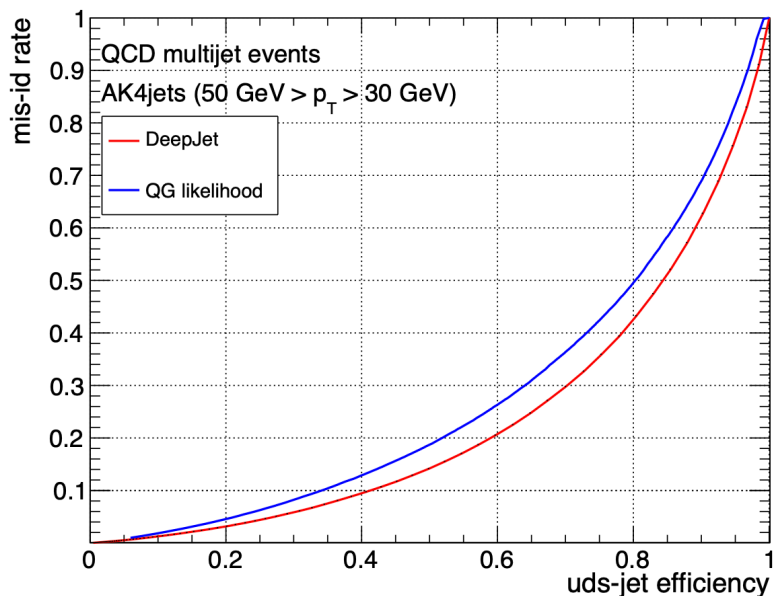


[[CMS-DP-2020-002](#)]

(13 TeV)

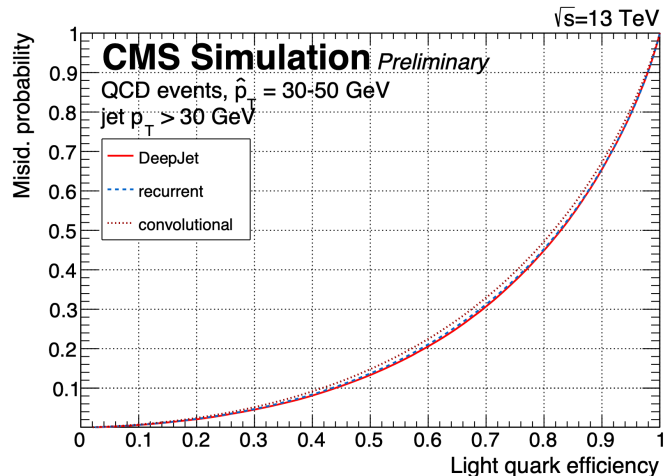


- DeepJet: Deep neural network algorithm
 - 16(8) properties of up to 25 charged (neutral) particle-flow jet constituents
 - 12 properties of up to 4 secondary vertices associated with the jet



- 2 Comparable approaches to DeepJet [CMS-DP-2017-027]

Long short-term memory (LSTM)



DeepJet

[CMS DP 2017-027](https://cds.cern.ch/record/2275226)
cds.cern.ch/record/2275226

↓ NN approaches compared to DeepJet in Quark/Gluon discrimination [Quark:light*]:

recurrent [inspired by arXiv:1702.00748]: Input: **relative $p_T/\eta/\phi$** and PUPPI (Pileup Per Particle Identification) **weight** (arXiv:1407.6013) of **charged** (fed to one recurrent layer of 100 nodes - LSTM) and **neutral PF cand.** (fed to identical layer). LSTM output then merged with **global*** variables in a dense NN [1 layer of 200 nodes, 5 of 100].

convolutional: Jet treated as image on $\eta - \phi$ plane. 3rd dimension - **color**: (separate study for charged and neutral PF cand.) **relative p_T** and **particle multiplicity** within the pixel. This input info fed to a CNN (Convolutional NN) [as in arXiv:1612.01551], then merged with the **global*** variables in a dense layer of 128 nodes.

Part of figure from arXiv:1612.01551

CMS Simulation Preliminary
 QCD events, $\sqrt{s} = 13$ TeV, Phase 1
 jet $p_T > 70$ GeV
 AK4 jets

Misid. probability

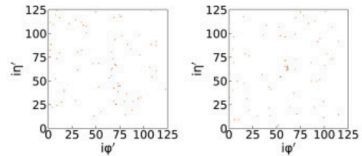
correct light jet identification prob. → light quark efficiency

*Jet variables:
 jet p_T/η ,
 #(charged PF cand.),
 #(neutral PF cand.),
 #(SV within the jet)

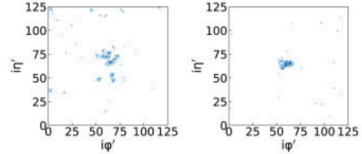
[Jets originating from gluon splitting to bb or cc not considered as gluon jets]

➤ Similar performance among DeepJet and 2 alternative approaches

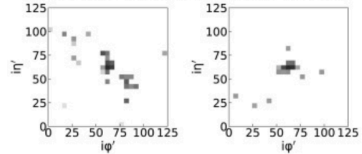
- End-to-end jet classification
[\[NIM A 977 \(2020\) 164304\]](#)



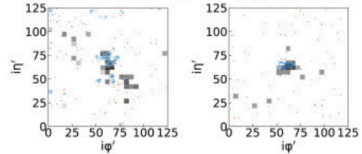
(a) Tracks channel. Left: gluon jet, Right: quark jet.



(b) ECAL channel. Left: gluon jet, Right: quark jet.



(c) HCAL channel. Left: gluon jet, Right: quark jet.



(d) Composite jet image. Left: gluon jet, Right: quark jet.

